PHASE CONJUGATE PROPAGATION STUDY

G.J. Dunning, M.L. Minden, D.M. Pepper
Hughes Research Laboratories
3011 Malibu Canyon Road
Malibu, California 90265

C. Oh, K.T. Andrews, E.S. Fry
Texas A&M University
Dept. of Physics
College Station, Texas 77843-4242

DTIC
ELECTE
SEP 27 1995
S D
B

October 1994
Final Report

Contract Number: N00014-93-C-0011
January 1992 through December 1993

Office of Naval Research
Code: 126
Ballston Tower One
800 North Quincy Street
Arlington, VA 22217-5000
Attn: William Stachnik

19950925 053

DISTRIBUTION STATEMENT A
Approved for public release;
Distribution Unlimited

DTIC QUALITY INSPECTED 5

94 11 3 061

REPORT DOCUMENTATION PAGE

Form Approved
OMB No. 0704-0188

Public reporting for this collection of information is estimated to average 1 hour per response, including the time for reviewing instructions, searching existing data sources, gathering and maintaining the data needed, and completing and reviewing the collection of information. Send comments regarding this burden estimate or any other aspect of this collection of information, including suggestions for reducing this burden, to Washington Headquarters Services, Directorate for Information Operations and Reports, 1215 Jefferson Davis Highway, Suite 1204, Arlington, VA 22202-4302, and to the Office of Management and Budget, Paperwork Reduction Project (0704-0188), Washington, DC 20503.

1. AGENCY USE ONLY (Leave Blank)	2. REPORT DATE	3. REPORT TYPE AND DATES COVERED
	October 1994	Final Report Jan. 92 - Dec. 93

4. TITLE AND SUBTITLE

PHASE CONJUGATE PROPAGATION STUDY

5. FUNDING NUMBERS

N00014-93-C-0011

6. AUTHOR(S)

G.J. Dunning, M.L. Minden, D.M. Pepper
C. Oh, K.T. Andrews, E.S. Fry

7. PERFORMING ORGANIZATION NAME(S) AND ADDRESS(ES)

Hughes Aircraft Company
Research Laboratories
3011 Malibu Canyon Road
Malibu, CA 90265

Texas A&M University
Dept. of Physics
College Station, TX 77843

8. PERFORMING ORGANIZATION REPORT NUMBER

94M-0587/J6431

9. SPONSORING/MONITORING AGENCY NAME(S) AND ADDRESS(ES)

Office of Naval Research
Ballston Tower One
800 North Quincy Street
Arlington, VA 22217-5000

Attn: William Stachnik
Code: 126

10. SPONSORING/MONITORING AGENCY REPORT NUMBER

11. SUPPLEMENTARY NOTES

12a. DISTRIBUTION/AVAILABILITY STATEMENT

See DoD D5230.4 "Distribution Statements on Technical Documents"

12b. DISTRIBUTION CODE

13. ABSTRACT (maximum 200 words)

This study addresses two issues that relate to optical communication systems over a propagation path that includes an ensemble of randomly distributed dynamically moving scattering sites. One issue pertains to the reduction of off-axis scattering experienced by a probe beam of light that propagates from a remote sensor to an interrogator over the path. A second issue involves the sensing and quantification of any global motion of the scattering sites in the presence of background, random motion. Through the use of nonlinear optical phase conjugation techniques, a wavefront-reversed replica of an incident probe beam can be realized that reduces off-axis scattering on its return transit through a medium and, at the same time, senses the presence of global phase shifts due to a net motion of an otherwise randomly moving ensemble of scatterers.

14. SUBJECT TERMS

Laser Beams, Nonlinear Optics, Optical Communication, Phase Conjugate Mirrors, Phase Conjugation, Scattering, Propagation, Remote Sensors, Propagation Compensation

15. NUMBER OF PAGES

54

16. PRICE CODE

17. SECURITY CLASSIFICATION OF REPORT	18. SECURITY CLASSIFICATION OF THIS PAGE	19. SECURITY CLASSIFICATION OF ABSTRACT	20. LIMITATION OF ABSTRACT
Unclassified	Unclassified	Unclassified	

"PHASE-CONJUGATE PROPAGATION STUDY"

TABLE OF CONTENTS

Accession For
NTIS GRA&I ☑
DTIC TAB ☐
Unannounced ☐
Justification
By per letter
Distribution/
Availability Codes
Dist | Avail and/or Special
A-1

"PHASE-CONJUGATE PROPAGATION STUDY"

LIST OF FIGURES

"PHASE-CONJUGATE PROPAGATION STUDY"

LIST OF FIGURES

"PHASE-CONJUGATE PROPAGATION STUDY"

1.0 INTRODUCTION AND SUMMARY

Hughes Research Laboratories (HRL), a division of Hughes Aircraft Company, is pleased to present this final report on an ONR program (contract number N00014-93-C-0011) entitled "Phase-Conjugate Propagation Study." The overall goal of this study was to explore various underwater optically based scenarios including those pertaining to communication links and remote sensing applications and to experimentally address related implementation issues. In the communication application, for example, it is desirable to realize a high-bandwidth optical uplink which emanates from a submerged platform, with autoalignment capability to enable tracking of a given interrogator (which may be submerged or above the surface), with high detection efficiency by the desired party and concomitantly, with low probability of interception and/or detection (LPI/D) by undesirable third parties (friendly or otherwise). In the remote sensing case, as an example, a means is required by which one can detect and quantify the global motion of water-borne colloidal suspensions for various metrology applications, in the presence of random (e.g., Brownian) motion, also, with LPI/D and with high system photon efficiency.

Both of these optically based scenarios are subject to real-world adverse environmental affects, which, if not properly addressed, could otherwise degrade the performance of the given system at best or, in some cases, compromise the ability of the system to function at all. It was therefore paramount to not only conceive of architectures which can lead to satisfying the desired applications but, also, to experimentally demonstrate various means by which key environmental issues can be successfully overcome.

Environmental issues such as large-scale and small-scale dynamic scattering (with scale dimensions relative to the wavelength of light), as well as time-varying relative platform motion, all present formidable challenges to the successful implementation and operation of the above-mentioned systems. Examples of these deleterious, randomly occurring perturbations include centimeter-sized underwater density fluctuations, micron-scale size bubbles, various submerged biological lifeforms, and air-water interface optical distortions and wave motion.

In this report, we first discuss an overview of the project in this section, followed in subsequent sections by background details and motivations, experimental results on the various tasks and, finally, we conclude with our insights gained and

recommendations for future efforts.

Under this program, we have identified methods by which one can potentially improve the performance of the above-mentioned applications under these real-world conditions and, in selected cases, we have performed proof-of-concept experiments to validate our conjectures. To this end, we explored two key areas of concern, which form the pair of tasks that comprised this effort: (1) how to realize an optical beam that undergoes a minimal amount of scattering as it propagates through various suspensions while, at the same time, enabling coherent detection of any encoded information impressed upon the beam; and (2) how to remotely measure the global velocity component from a collection of suspended particles, which may also possess a differential motion. A concern common to both of these needs is that one also desires to perform the respective operations with minimal photon flux and with minimal third-party detection.

We have identified conditions by which these methods can be employed, including those relating to the nature of the scattering centers (transparent and translucent dielectric media; absorbing media), their environment (stationary and dynamic suspensions), and well as the optical resolution and response time (spatial and temporal bandwidths, respectively) of the system.

To explore the systems issues alluded to above, we have identified and shown that an optical technique — nonlinear optical phase conjugation, NOPC[1,2] — has the potential of addressing both of these key issues and, moreover, can also lead to many other related systems implementations. In NOPC, an all-optical real-time holographic technique is used to compensate for various propagation-path distortions, including atmospheric turbulence, aberrations in laser gain media and optical components, beam wander, and modal dispersion in guided-wave structures, to mention a few. The basic notion of the classic NOPC approach is that a wavefront-reversed replica — often referred to loosely as a "time-reversed replica" — can be generated that, in essence, "undoes" the path distortions experienced by a given incident probe wave upon its reverse passage through the same (reciprocal) distortion medium. So long as the medium is essentially stationary during the optical propagation time and the response time of the NOPC generation element (termed a phase-conjugate mirror), then the scheme can function quite effectively. One fundamental requirement for this approach to function, however, is that all of the phase-distortion information experienced by the probe wave must be collected in order for the wavefront-reversed replica to ideally correct for the path aberrations. As less information — for example, scattered light — is collected, the ability for the conjugate beam to "undo" the path-induced phase errors becomes degraded (the precise degree of degradation depends on the nature of the distortion and the geometry of the system, etc.).

In the case of path distortions, or losses, created by optical scattering, it has been conventional wisdom that unless all the light is collected, perfect reconstruction of the incident wavefront cannot be realized. This conjecture makes intuitive sense when viewed from a time-reversal perspective: If an incident plane wave undergoes scattering by nonabsorbing centers and emerges from the volume as a highly distorted wave in many directions, then, if one can collect all of the light and time-reverse all components of this highly complex beam, then the time-reversed replica will "undo" the distortions and emerge from the volume, with its wavefront restored to that of a plane wave.

Although the above picture is theoretically accurate, its conclusion does not necessarily apply to some of the communication and remote sensor issues under consideration for this study: Namely, how one can reduce the effects of scattering losses in a two-way communications link — especially if not all of the scattered light is collected by the conjugator or if the scattered light is not processed by the conjugator — and, at the same time, give rise to a returned wavefront which matches (even approximately) that of its incident counterpart.

Based on our previous experience with retromodulators[3,4] in underwater scenarios[4] using optical phase-conjugate mirrors, we have observed evidence that, indeed, the phase-conjugate return appeared to undergo less scattering losses than its forward-going counterpart (i.e., the incident probe beam that initially sampled the distortions) — even if a limited amount of the light was collected by or processed by the conjugator. This rather counter-intuitive result appears to apply in many cases of practical interest regardless of the nature of the scatterers: phase-only (e.g., dielectric) scatterers as well as absorbing "scattering sites" can be employed in this scenario.

Our hypothesis, which is consistent with this interesting finding, is that if conjugate wave avoids, or "misses," the scattering sites on its reverse passage through scattering medium, then less scattering will be experienced relative to that of the incident wave. In other words, the argument seems to involve the requirement of the conjugate beam to both spatially resolve and temporally track the scattering site "boundaries," or "external shape," rather than require (the more stringent condition) that all of the scattered light be collected (with no absorption) and the wavefront reversed. It was this conjecture that led to the present program: Namely, to perform a more precise set of experiments to quantify this effect — in both static and dynamic scattering media — and, moreover, to demonstrate the ability of the detected backward-going wave to match the wavefront of its incident beam.

If the above conditions can be (even approximately) realized — and below, we show evidence that this is, indeed, the case — then a coherent detection approach can be employed to sense any signals encoded onto the return beam. It turns out that the encoded signal can result from several different sources. In one case, the beam at

the conjugator's location can be modulated, thereby forming a retromodulator communications link with minimal scattering losses on the returned beam. In another case, the scattering sites themselves can be temporally modulated via a global phase shift. In the latter case, the ensemble can be viewed as a distributed remote sensor.

Our program addresses both of these scenarios in part. The first task involves quantifying scattering losses as a function of angle and polarization. The second task addresses the ability of a conjugate wave to sense global motions of an ensemble of scattering sites — with the added benefit of also reducing the scattered component of the detected beam. Preliminary results indicate that both of these desirable properties can be realized through the use of a phase-conjugate optical architecture. These successful results can therefore lead one to consider construction of an actual two-way coherent-detection communications link, and also a sensor for remote sounding measurements — both with reduced scattering losses, as well as with high-bandwidth and high-sensitivity performance.

In the sections that follow, we describe in detail our experimental efforts as well as the motivations behind them, our conclusions, and our recommendations for future follow-on efforts to address outstanding issues which we have identified throughout the course of this program. In the remainder of this section, we summarize our findings at an executive level as an aid to the reader. As discussed above, the basic approach which we have employed to deal with the system needs and the environmental issues alluded to above involves the use of optical compensation techniques, such as nonlinear optical phase conjugation (NOPC). NOPC employs all-optical methods to realize real-time holographic processing of complex, dynamic, spatial and temporal wavefront information — which an optical beam can experience upon propagation through turbulent, highly scattering paths. Free from complex electro-mechanical intensive hardware and associated computer-intensive algorithms, NOPC techniques offer a compact, fast-responding parallel processing approach by which one can address a multitude of optical propagation problems, including dynamic distortion effects, tilt errors, and scattering effects. By employing optical phase conjugation techniques, we have been able to invent, address and demonstrate the following:

- Reduction in scattering losses induced by a stationary glass cylinder by a factor of 2 to 5, using a phase-conjugate optical beam relative to a nonconjugate beam, measured as a function of incident angle and polarization.

- Ability of a self-pumped photorefractive-based phase-conjugate mirror to track global transverse motion of moving scattering sites across its field-of-view — a necessary condition to reduce scattering from the ensemble.

- Reduction in scattering losses induced by a dynamic colloidal suspension of dielectric microspheres in an aqueous solution by a factor of 2, using a phase-conjugate optical beam relative to a tilt-corrected nonconjugate beam, measured as a function of incident angle through 5 to 10 cm length cells.

- Improvement in the transmission of unscattered light through a dynamic colloidal suspension of dielectric microspheres in an aqueous solution by 43%, approaching complete compensation for scattering losses, using a phase-conjugate beam relative to a tilt-corrected nonconjugate beam, through a 1 mm cell.

- Ability of a phase-conjugate signal to be wavefront-matched to an optical local reference beam in the above geometries, thereby enabling the option of establishing a coherent detection link with high photon efficiency.

- Invention of an optical system architecture using a self-pumped phase-conjugate mirror to enable remote sensing of the global motion component of a collection of suspended scattering sites, in the presence of random differential motion within the ensemble. In the process the received interrogation beam possesses a phased-up return from the scattering sites so that coherent detection techniques can be employed for post-processing of the information. The system, at the same time, also minimizes propagation losses through the ensemble via reduction of the scattering.

- Improvement in the signal-to-noise performance of a remote sensor to detect global motion of a colloidal suspension in the presence of random differential motion using a phase-conjugate optical beam relative to a tilt-corrected nonconjugate beam, measured at an angle normal to the plane of incidence, and employing the above-mentioned invention.

In order to realize these results, we have constructed an optical test apparatus consisting of a goniometer, with dual-polarization measurement capability over angular ranges both parallel and normal to the plane of incidence, as defined by the input beam and the reference beams in the system. An argon-ion laser at 514.5 nm served as the optical source for our measurements, while a barium titanate crystal was employed as a phase-conjugate mirror, configured in the so-called "cat" arrangement, thereby serving as a self-pumped conjugator. This basic apparatus was employed for both the detailed angular and polarization-dependent scattering measurements, as well as for the remote sensor experiments.

To facilitate a well-defined fixed-scattering system, a quartz optical fiber was employed as a side-scatterer in the stationary scattering studies, while single- as well as dual-sized colloidal suspension scattering cells were fabricated for the dynamic scattering measurements. To make the dynamic measurements, a collection of scattering cells have been prepared, consisting of varying lengths, containing a variety of different sized dielectric (e.g., polystyrene) and metallized (precision ball bearings) spheres of differing densities, and employing various host liquids such as water and glycerin. In the case of the stationary scattering site measurements, free-space beam combining was used to realize a heterodyne detection system. In the dynamic scattering experiments, optical fiber beam combiners served as a means to perform the coherent detection system, with the phase-conjugate behavior (in both cases) enabling wavefront-matching of the pair of beams. The scattering cells were mounted in our apparatus in both vertical and horizontal orientations (defined as the direction of the cylindrical axis of the cell relative to the horizontal table surface). This enabled studies to be made regarding the settling of the suspended particles: in the vertical cell orientation, the particles would fall along the direction of the main laser beam; in the horizontal cell orientation, the particles would fall "through" the beam and, eventually, out of the beam path.

Finally, a suite of diagnostic detectors were employed to characterize the performance of our systems under study, including far-field photodetectors, video-based imaging sensors (e.g., CCD's) for visualizing the scattering sites, and optical heterodyne detectors, lock-in amplifiers, and spectrum analyzers for the remote sensor experiments.

In the next section, we describe our experimental apparatus and results in detail. The notion of using phase-conjugation techniques for these various systems was initially conceived at HRL. The overall program was managed at HRL with the experimental work performed at HRL, with a subtask performed at Texas A&M University. Texas A&M was also involved with assisting with the preparation of scattering cells employed throughout the program. The technical dialog established between HRL and Texas A&M proved to be extremely useful to the success of this program.

The experiments on the reduction of scattering via phase-conjugate beams are discussed first, followed by the experiments on the remote sensing of global phase shifts using a phase-conjugate architecture. In the scatter-reduction experiments, two different dielectric scattering systems were considered. In one set of experiments — which were performed at Texas A&M University, by C. Oh and K.T. Andrews, under the direction of Professor E.S. Fry — a fixed (i.e., stationary) single scattering site was employed, consisting of a quartz optical fiber segment. The fiber was illuminated in a "broadside" manner by a probe beam (with a spot circular in cross section). That is,

the axis of the fiber section lies in a plane normal to the optical beam propagation vector.

In another set of scattering experiments — which were performed within the Optical Physics Laboratory at HRL by G.J. Dunning, M.L. Minden, and D.M. Pepper — suspensions of dynamically moving scattering sites were employed, consisting of polystyrene microspheres of differing diameters submerged in water and other host liquids. Cells of various lengths and containing a variety of fill concentrations were used in these experiments.

The work on the remote sensor experiments — the second task on this effort — was performed at HRL by the same personnel mentioned above. In these experiments, scattering cells using a variety of suspended scattering sites were employed, with global motion introduced to the ensemble of sites via transducers attached to the walls of the respective cells.

In summary, we have demonstrated techniques by which one can realize a laser-based optical channel with reasonable efficiency, reduced off-axis scattering losses, and the capability for coherent detection of the information to be relayed. Such systems can be exploited for communications applications, as well as for remote sensing operations — all with improved performance relative to present-day approaches, and with robustness to perform under real-world conditions with minimal hardware and post-processing. The HRL authors acknowledge fruitful discussions with R.N. Schwartz, P.V. Mitchell, M.B. Klein, T.R. O'Meara, H.W. Bruesselbach, R. Chapman, and R.V. Harold.

2.0 BACKGROUND

2.1 Scattering Reduction using Phase-Conjugate Beams

The motivation to reduce scattering from an ensemble of randomly situated and dynamically moving sites has obvious implications on improving the performance of an optical communications link as well as on the ability to reduce the possibility of undesirable detection of the information. In the former case, a greater photon flux can be detected at the receiver over a finite field-of-view if scattering along the propagation path can be reduced. Moreover, if a phase-conjugate[1,2] communications system[3,4] can be realized (defined at the end of this paragraph), then several additional advantages can be achieved: (1) the return is autoaligned with the interrogator, enabling a tracking and pointing operation to ensue in real-time; (2) propagation-path errors can be compensated by the return beam, reducing losses; and (3) wavefront-matching with an optical local oscillator can be realized, enabling efficient coherent detection of the returned signal. Of these benefits, perhaps the third advantage is the most relevant in terms of improving the link performance of typical scenarios. A sequence of events typical of an optical link considered here is as follows: (1) first, an interrogator probes a region where a remote sensor (which contains a phase-conjugate mirror) is situated; (2) second, the remote site optical collection system directs the now-received interrogation beam onto a phase-conjugate mirror; (3) the beam is encoded at the remote-site location (via phase, amplitude, etc.); (4) the phase-conjugate return, encoded with the desired information, retraverses the incident path, and propagates back to the location of the interrogator.

It is well known that a phase-conjugate return can perfectly correct for path distortions if all the scattered light is collected and ideally conjugated.[1,2] For this to be the case, the wavefront-reversed replica must contain all the spatial frequencies present in the received beam for complete compensation. In this case, the return beam, after double-passing the reciprocal distortion (assuming that the distortion remains essentially stationary during the reverse transit time and the response time of the conjugator), will emerge with its wavefront completely restored, as if the distortion never existed in the first place. In this ideal case, a perfect communication channel can be realized, as if the optical beam traversed a "vacuum path" linking stationary stations. As such, no scattering would be experienced by the return beam under these ideal conditions.

However, in the case where not all of the light is collected — either by virtue of scattering beyond the field-of-view of the receiver or if the scattering sites are absorbing — then, conventional wisdom may conclude that the return beam will not

emerge with its initial wavefront restored after a double-pass of the path distortion. Although this conjecture is indeed correct, for the two system issues at hand, however — namely, the reduction of scattering and coherent detection of the return link — a conjugate-based system can realize enhanced performance, even in the case of incomplete collection of the light.

The reason for these improvements — scatter reduction and wavefront reconstruction — can be garnered from the following argument: If one assumes that the forward-going beam has been scattered by the various sites in its path then, in order to realize a return beam that does not undergo scattering, a sufficient requirement is that it merely "avoid" the scattering sites during its reverse transit. That is, if one views the forward-going beam at the phase-conjugate mirror as possessing "shadows," or dark regions, created by the scattering sites, then so long as the return wave faithfully reproduces the same shadows at the same spatial locations as where the scattering sites are located, the return-wave will then effectively avoid, or "miss," striking the respective sites and, therefore, avoid being scattered by them (again, assuming that the sites remain essentially fixed in space during the round-trip transit time to and from their location and, moreover, during the response time of the conjugator). On the other hand, a nonconjugate wave will not exactly reproduce the shadows created by the scatterers and, therefore, will experience finite scattering by them during its return transit.

Since the conjugate wave also reproduces its phasefronts at the plane of the scattering sites, the beam which then passes back toward the receiver from this plane will have its phasefronts intact, except for the "holes" induced by virtue of the sites. The beam which finds its way back to the detector at the interrogator location will therefore have its phasefront approximately matched to that of the beam which initially emanated from that location, except for some side lobes induced by virtue of the absence of some photons, which were "masked out" by the scattering sites (during the initial pass). Although it is not proved here, it appears intuitive that this phasefront (even with "holes" in the beam induced by the scattered light on the forward pass) is probably just as efficient (if not more so) for coherent detection than any other wavefront which would have propagated through the scattering path. Note that this discussion applies to both stationary, as well as to dynamic ensembles of scatterers.

There is yet another picture by which one can view the interaction which would lead to a reduction in scattering: by conjugating and time-reversing only the so-called "ballistic" or "snake-like" components[5] of the incident beam, then the scattering experienced by the return wave could be reduced, if not eliminated. It has been discussed in the recent literature that one can image through highly scattering media by processing only that component of the light which has not undergone any scattering (or, in the worst case, has undergone essentially minimal forward

scattering). These components have been referred to, respectively, as ballistic and snake-like, in nature. In essence, these two components can be viewed as photons which have essentially missed, or avoided, being scattered upon passage through the propagation path. Therefore, any image-bearing information can, in principle, be recognizable after collection of these selected photons. Typically, these photons arrive earliest in time, so various gating and coherence techniques have been employed by workers in the field to separate them from the background of highly scattered light. In addition, in the case of dynamically scattering media, motion-induced frequency effects (differential Doppler shifts) can be used to advantage in distinguishing the background (undesirable) scattered light from the unshifted, (desired) ballistic component.[6] Therefore, nature has assisted us in "frequency tagging" the undesirable components in this case. Although this latter condition can be highly exploited in many scenarios, it appears to be, nonetheless, not fundamental.

In our case, so long as we can selectively conjugate only these ballistic and snake-like photons, then the wavefront-reversed replica will pass back through the medium with reduced scattering. In order to most effectively process this information, one has to spatially resolve the only the "outline," or external boundary regions of the scattering sites through which the ballistic and snake-like components propagate — and, not necessarily, the detailed features within the sites themselves. In essence, it is these photons which will retraverse the medium without scattering.

Based on the above discussions, the fundamental requirements for reduction of scattering appear to be the following: (1) the conjugate-wave must resolve (i.e., reproduce) the transverse dimensions of the scattering sites upon reverse transit; (2) the conjugator must respond fast enough to "track" transverse motion of the scattering sites; (3) the depth-of-focus of the system must be adequate to resolve the longitudinal feature(s) of the scattering sites; (4) the system must resolve these features within the entire volume (both transverse and longitudinal) containing the scattering centers; and (5) the transverse and longitudinal motion of the sites relative to its size must be small during the photon transit time and the conjugator response time.

The system performance would degrade as multiple "shadows" are realized (e.g., multiple scattering events) whose scale sizes exceed the resolving power of the system. Put another way, if the shadows cannot be reconstructed by the system (optics and conjugator), the conjugate wave itself will experience scattering and wavefront distortions scattering upon its reverse transit. This state-of-affairs can lead to a degradation of the system performance — both in terms of reduced scattering and, moreover, in the case of a coherent detection system, where one desires that the return beam be wavefront-matched to that of an optical local oscillator beam.

As we describe in Section 3 below, we have observed a reduction in the

scattering of a conjugate wave relative to a nonconjugate wave under various conditions. Experiments were performed using fixed scattering sites and also using cells containing dynamic scattering centers. In the latter case, measurements were made for microspheres whose spatial extent was both unresolvable as well as resolvable by our system.

We conclude this section with a listing of several examples of scattering sites, whose scattering can be reduced via phase conjugation processes. In all cases, spatial resolution requirements apply to the entire volume of sites. For simplicity, we neglect depolarization effects, which can also be present:

- *Highly translucent, stationary scattering sites:*

Significant reduction of scattering in this case requires collection and conjugation of all the scattered light. That is, the system needs to spatially resolve the entire bandwidth of the scatterer, including its internal spatial features. This case is therefore the most demanding in terms of optical collection issues, owing to the detailed spatial structure, which gives rise to large-angle scattering. We define translucent as particles possessing spatial structure on the order of the wavelength of light or less.

- *Highly transparent, stationary scattering sites:*

Significant reduction of scattering in this case also requires collection and conjugation of all the scattered light. Here too, the system needs to spatially resolve the entire bandwidth of the scatterer, including its internal spatial features. This case is still quite demanding in terms of optical collection issues, since any internal spatial features will result in large-angle scattering.

- *Highly transparent or translucent, dynamic scattering sites:*

Significant reduction of scattering in both of these cases can be achieved via selective conjugation of the ballistic and snake-like components of the light. Owing to the differential Doppler shifts experienced by the nonballistic and nonsnake-like (i.e., scattering) components of the light, so long as conjugator respond to only the slowly varying phase components of the light (and, therefore, avoid conjugating the "frequency tagged" light, which labels the highly scattered photons), then the backward-going beam will be minimally scattered. This notion has been employed in a compensated one-way imaging scheme.[6] In this case, a slow-responding conjugator can be employed that need not "track" the differential Doppler-shifted components. As such the spatial bandwidth requirement is that the system need only resolve the exterior boundary of the scattering sites (as long as the amplitude of the spatial fluctuations is small relative to the size of the particle, which is typical for

Brownian motion), and resolve slow drifts induced, for example, by global currents.

- *Highly absorbing (i.e., opaque), stationary scattering sites:*

Significant reduction of scattering in this case requires that the conjugator spatially resolve the exterior features (i.e., the boundaries) of the scattering sites. This case mimics that of the lensless imaging application of phase conjugation in the case of binary amplitude masks (zero and 100% transmission features).

- *Highly absorbing (i.e., opaque), dynamic scattering sites:*

Similar to the stationary, absorbing case above, significant reduction of scattering in this case requires that the conjugator spatially resolve the exterior features of the scattering sites, subject to small-amplitude fluctuations relative to its size. Owing to the differential Doppler motion, a slow responding conjugator (as in the above-mentioned dynamic scattering cases) can also assist in selectively conjugating only the ballistic and snake-like components of the unscattered incident light. This case appears to be the least demanding situation relative to the other cases.

2.2 Remote Sensing of Global Scattering-Site Motion

The ability to sense the global motion component of a dynamic ensemble comprised of arbitrarily moving (e.g., experiencing differential Doppler motion), randomly sized and distributed scattering sites has profound implications in myriad communication, industrial, and medical applications. An example may be the need to sense the global velocity component in a water-borne colloidal suspension undergoing noise in the form of Brownian motion — the noise of which may otherwise corrupt the ability of a coherent remote sensor from functioning up to its theoretical sensitivity limit in the best case, or nonfunctional in the worst.

We note that, in principle, an array of sensors can be used to sense the desired global motion component of an ensemble, while compensating for differential motion experienced within the suspension. Such arrays, along with the required post-processing can quickly become intractable, especially in the case of large arrays of scatterers. In order to most efficiently ascertain the global component of the motion with high precision and with good overall performance, one must sample the motion — differential and global — of all the sites. This implies that an individual detector be employed for each scattering site, so that the number of detectors match the number of sites, which is consistent with the Nyquist condition. This state-of-affairs quickly become impractical for large numbers of sites. For example, one million sites would require an array of one million sensors, with the requisite post-processing algorithms.

Through the use of a phase-conjugate architecture, the system can improve the

current signal-to-noise ratio of this class of remote sensor by several orders of magnitude and, moreover, dramatically simplify the complex receiver hardware and signal processing that is currently employed. In the best case, one can reduce the sensor complexity from a receiver array consisting of over one million detectors (and associated post-processing) to a *single* detector element. Our basic philosophy to approaching this sensor is an outgrowth of the experimental insights that led to the results on the above task — namely, that a phase-conjugate wave has the potential to propagate through a highly scattering distributed medium with minimal scattering relative to a non-conjugate beam and with the ability to phase-up the resultant conjugate wave so that the initial wavefront can be (approximately) recovered.

The basic idea behind the operation of this sensor is the following: an "ideal" phase-conjugate mirror will, by virtue of its "time-reversed" wave generation, effectively "undo" all phase distortions. In the case of a combination of global and differential motion of an ensemble of scattering sites, an "ideal" conjugate beam will, upon double-passing the suspension, return a probe beam free of all phase information — therefore, no details of the motion is obtained. This follows from the "time-reversal" properties of the conjugation process.

However, in the case of a *self-pumped* conjugator, all details of any *global* motion are preserved, since it is, in essence, a self-referencing device. In this manner, it behaves as an ordinary mirror. In addition, since it phases up all the scattered beams in a double-pass architecture, the returned probe beam is free of all differential phase distortions. These phase distortions can be the result of stationary scattering sites randomly situated in space (giving rise to differential, yet fixed, phase distortions), as well as the result of sites whose locations vary randomly in time (differential, yet dynamic, phase distortions). In either case, net phase changes, if any, are preserved by the self-pumped phase conjugator upon its return pass. In actuality, the net phase shift is doubled upon detection by virtue of the second pass through the system.

The requirements for this class of sensor to properly function are, apparently, the following: (1) the system must spatially resolve the size of the scattering sites for most efficient operation; (2) the conjugator must be able to temporally resolve the differential component of the ensemble motion; and (3) the spatial location of the scattering sites remain essentially the same during the photon round-trip time as well as during the response time of the self-pumped conjugator. Under these conditions, the conjugator should preserve the global phase shifts (assuming that they are small compared to a wave) even though they may exceed the temporal bandwidth of the grating formation timescale.

The above conjecture (which we state without proof) follows intuitively given the fact that once the real-time gratings form (within the conjugator) to track any differential motion, the remaining component (the global phase shift) will present a minor

perturbation on the location of the overall fringe pattern, yet, the general shape of the pattern will remain the same (assuming that there is no significant diffraction occurring over the transverse fringe shift). We note that, indeed, laser ultrasonic interferometric sensors have been successfully operated using self-pumped conjugators to compensate for surface speckle (which can be viewed as giving rise to differential, yet fixed, phase distortions); however, although this demonstration was successful, it may be a major extension of the concept to include dynamic temporally varying differential phase distortions, which, in the present case, occur over a volume, and not just on a surface. Nonetheless, the experimental evidence presented below substantiates the validity of the concept — at least, under our experimental albeit, limited, parameter space.

To further motivate the need for an enhanced sensor system and to illustrate how one may implement our sensor enhancement technique, we will consider the limitations present in a bistatic remote laser sensor system. A typical geometry consists of a laser probe beam which is directed towards a small region of space, with the goal to measure global temporal fluctuations in the sample volume. The sample volume contains a collection of scattering sites (such as water-borne particles) in a colloidal suspension which, in the presence of a global fluctuation, undergoes a net motion. The goal of the sensor is to detect this global component. A fraction of the optical probe beam light is scattered from these particles, with yet a smaller fraction of the scattered light collected by an optical receiver, which is situated in close proximity to the transmitter. The ensemble of scatter sites behaves as a distributed, albeit inefficient and noisy, thinned-array remote sensor. The result of the net global fluctuation is manifested by a concomitant net phase shift in the received probe beam. The optical receiver can then infer the global fluctuation by various coherent detection, sampling, and post-processing techniques.

Several key interrelated factors severely limit the performance of existing, conventional systems and devices this class of remote sensor. One factor relates to Brownian motion of the colloidal suspension, which is a fundamental property the system. This particle motion results in random Doppler shifts imposed on the return beam. Since the collected light for the sensor stems from scattering of a probe beam by these randomly moving sites, the raw receiver signal consists of an uncorrelated (Brownian) noise spectrum superimposed upon the desired information, which consists of an overall global Doppler shift of the ensemble. This state-of-affairs is exacerbated by the fact that the amplitude of the desired (spatially global) information is typically less than that of the Brownian-motion-induced noise. Moreover, the noise spectrum of the uncorrelated background typically lies within the spectral band of the desired information.

A related problem which can adversely affect the performance of present-day

remote sensors is the fact that the received signal has a dynamic and spatially "speckled" appearance. That is, the as-received beam has gross intensity fluctuations across the aperture of typical wide field-of-view collection systems. The dynamic speckle is due to the fact that the scattering sites are randomly situated in the suspension and in constant motion. Therefore, there is a loss of spatial coherence in the raw detected light. This property of the system places stringent requirements on the detector hardware, its dynamic range, and post-processing algorithms needed to extract the desired signal.

A third factor that limits the performance of present systems stems from the fact that the scattering sites within the suspension typically have a relatively small cross section (both in terms of the physical size of the particles and in terms of its reflectivity) and also a small fill factor (i.e., a low number density). This results in a very low flux level at the receiver, which may approach that of the ambient background. Conventional optical amplifiers have limited utility here, since the gain required to detect the low-level scattered return beam can approach the parasitic limit (given the field-of-view, typical ranges, and practical laser illuminator fluxes). Another related problem is that most of the amplified light in a double-pass configuration merely passes "through" the ensemble of scattering sites without striking the scatterers. Thus, the overall system efficiency is typically very low and, in many cases, negates the utility of the remote sensor for many practical scenarios. This drawback also promotes third-party detection of the sensor source and location, which may not be desirable.

Another area of concern relates to the optical receiver and the required post-processing necessary to extract the desired signal information. Due to the highly speckled return, present sensor systems employ large detector arrays to collect light from individual speckles. During post-processing, the uncorrelated noise is averaged out, thereby extracting the desired coherent (global) motion of the ensemble of scattering sites. This procedure is extremely cumbersome, both in terms of the hardware (detector arrays approaching one million pixels, associated high-speed electronics, and computer modules), as well as the software algorithms.

Through the use of a self-pumped phase-conjugate system (combined with an optional high-gain amplifier placed upstream of the conjugator), one can realize a coherently phased received signal that forms constructively at the detector. In addition, the double-passed (and, optionally amplified) light will reform on, and thus "track" the scattering sites. This state-of-affairs minimizes optical losses due to light which would have otherwise "missed" the scattering sites on its return path (as is the case with conventional remote sensors), as well as to minimize third-party detection.

In order for our architecture to efficiently function, the conjugator must compensate for any spatial wavefront distortions arising upon reflection from the individual scattering particles, as well as the differential phase shifts between the

particles. At the same time, the conjugated beam must preserve the global motion and uniform phase shifts that carry the desired signal. The performance of the phase-conjugate enhanced system will, of course, be subject to the resolution, fidelity, and temporal response of the conjugator — requirements not unlike those of the above task, which addressed a related problem: the minimization of off-axis scattering by the ensemble.

There are several key objectives and issues to address in order to ascertain the merits of such an approach. One key objective, as we discuss below, is to demonstrate that a self-pumped conjugator can indeed compensate for, and effectively, remove the differential phase shifts detected from the scattering particles, while preserving the global phase shifts. In addition, other issues include the following: (1) the ability of a phase-conjugate interferometer to detect global frequency shifts which are superimposed in a broadband noise spectrum, thereby improving the signal-to-noise figure of the system; (2) the ability of a phase-conjugate system improve the overall system efficiency by minimizing off-axis scattering of the returned information; (3) the ability of a coherent detection system to function optimally by having the received wavefront match that of a local oscillator at the transceiver; (4) the change in system performance as the differential Doppler shifts exceed the spectral bandpass of the conjugator; and (5) the change in system performance as the scattering sites become unresolvable. We note that the last issue — spatial resolution and its effect on system performance — is common to both this task, as well as the above task (the minimization of off-axis scattering). On this program, we provided preliminary information on these issues, as we discuss in the next section.

3.0 TASK RESULTS

3.1 Scattering Measurements: Phase-conjugate vs. retro-reflected beams

On this task, we performed two sets of experiments, the results of which independently indicate that, indeed, a phase-conjugate beam minimizes off-axis scattering relative to that of a nonconjugate beam, even if the nonconjugate beam compensates for global tilts. The first set of experiments — which were performed at Texas A&M University by C. Oh and K.T. Andrews, under the direction of Professor E.S. Fry — involved the use of a fixed single scattering site, consisting of a stationary quartz optical fiber segment, which was illuminated "broadside" by a probe beam (circular in cross section). That is, the axis of the fiber section lies in a plane normal to the optical beam propagation vector. The second set of experiments — performed within the Optical Physics Laboratory at Hughes Research Laboratories by G.J. Dunning, M.L. Minden, and D.M. Pepper — employed a suspension of dynamically moving scattering sites, consisting of varying diameter polystyrene microspheres in water. In both cases, a goniometer was used to define a set of scattering angles about the respective sample, with heterodyne detection and phase-locking processing techniques employed to quantify the relative scattering flux. The phase-conjugate mirror in both sets of experiments consisted of a crystal of barium titanate, configured in the so-called "cat" geometry, resulting in a self-pumped conjugator. An argon-ion laser, operating at 514.5 nm, in a single longitudinal mode, and spatially filtered, was used as the source.

3.1.1 Static scattering experiments

3.1.1.1 Introduction

It is well known that phase conjugated light can correct the phase distortions introduced by a phase distorting medium.[1,2] There have been numerous experimental demonstrations of this phenomenon using various phase distorters and phase conjugating media.[7] Here, we report the experimental observations of this phenomenon using light scattering by a micron-sized particle. In an ideal case, if all the light scattered by a small particle is reflected back toward the particle by a phase conjugator, its phase should be corrected after interacting with the particle the second time; in principle, the incident wave would be recovered. In an experimental situation, generation of a phase conjugate reflection of all the scattered light is probably not reasonable, or of practical interest. Thus the precise form of the incident wave is

generally not recoverable. However, when light is scattered by a particle with radius larger than the wavelength, the scattering probability in the forward direction is so large that most of the scattered intensity is confined in the forward direction.[8] Therefore in practice we can approximately reproduce the ideal situation by phase conjugating a large portion of the forward scattered light. In the present work, a portion of the light scattered in the forward direction by a quartz fiber is retroreflected by a phase conjugator and re-scattered by the fiber. The angular distribution of this scattering is compared with that due to retroreflection by a normal mirror.

Based on the various classes of scattering sites discussed in Section 2.1, the present case falls under the category of a "highly transparent, stationary scattering site." As such, the requirement for the backward-going beam to reduce off-axis scattering demands that the system spatially resolve the scatterer, including its internal features. Therefore, the greater the field-of-view of the phase-conjugate mirror (assuming perfect wavefront reconstruction, or spatial fidelity), the more effective the system will be to reduce the scattering experienced by the conjugate return beam.

3.1.1.2 Experimental Apparatus

The experimental arrangements are schematically illustrated in Figures 1 and 2. A micron-size quartz fiber, whose axis is perpendicular to the plane of figure, is used as a scattering sample. The 514.5 nm line of a cw Ar^+ laser is polarized in the plane of incidence (plane of the figure). A 0°-cut $BaTiO_3$ crystal is used as a self-pumped phase conjugator.[9] The crystal is a cube whose edge dimension is approximately 5 mm, and its c-axis is in the plane of incidence. The intensities of the laser beam and the retroreflected beam are monitored throughout the experiment with detectors 2 and 1, respectively. The phase conjugate reflectivity of the crystal is estimated from these readings, and it was typically about 30% relative to the mirror reflection. The retroreflected light going back into the laser cavity is minimized by a neutral density filter. The angular distribution of the scattered light is measured with a photomultiplier tube (PMT) mounted on a rotating arm.

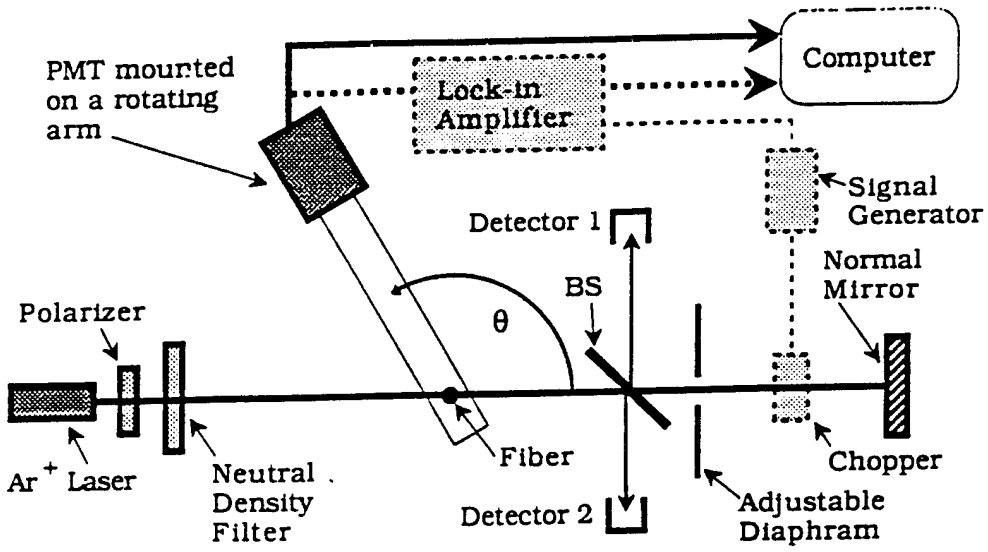

Figure 1. Apparatus schematic with normal mirror. The chopper and lock-in are used in the second set of experiments.

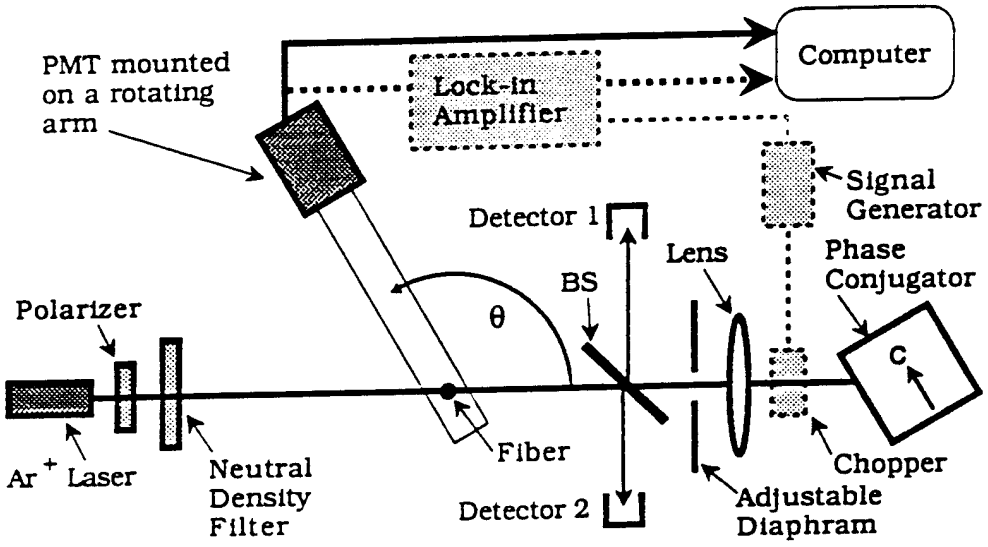

Figure 2. Apparatus schematic with phase conjugate mirror. The chopper and lock-in are used in the second set of experiments.

To calibrate the fiber size, the angular distribution of the scattered intensity is measured without a retroreflector and the radius of the fiber is determined by fitting this data to the theoretical calculations for the angular scattering function of an infinite dielectric cylinder.[8] For all the work to be described here, the fiber was a quartz cylinder with a radius of 19.8 μm. Two sets of experiments were performed. In the first set, the output of the photomultiplier was recorded directly by the computer and the data were then manipulated to separate the scattering by the incident and the retroreflected beams. In the second set, the retroreflected beam passed through a chopper and the photomultiplier output was processed by a lock-in amplifier tuned to the chopper frequency (as indicated by the dashed components in Figures 1 and 2). The lock-in output is proportional to the intensity of the light scattered from the retroreflected beam.

3.1.1.3 Experimental Results: Direct Measurements

Initially, the angular distribution of the scattered intensity is measured without a retroreflector. Both the light scattered in the forward direction and the incident laser beam are then retroreflected with a normal mirror, as shown in Figure 1, and the angular distribution of the scattered light is measured again. Since this first set of experiments does not employ the chopper, data for scattering from the retroreflected beam are obtained from these two angular distributions by subtracting the initial one from the latter one. Figure 3 shows the results for the 19.8 μm radius quartz fiber. Data for scattering from the incident laser beam (obtained in the absence of a retroreflected beam) are plotted as a function of scattering angle, θ. Data for scattering from the retroreflected beam (obtained by subtracting the two angular distributions) are plotted as a function of 180°-θ, so that forward scattering for the retroreflected beam can be easily compared to the incident beam scattering. As expected, the scattering of light reflected by a normal mirror has a structure almost identical to that produced by the incident laser beam. Due both to the reflections at the beam splitter and to the less than perfect reflection at the mirror, some light is lost; this accounts for the differences in amplitude. In addition, at the larger angles there are some anomalously large oscillations. With respect to these, we recall that the scattered intensity distribution observed with the phase conjugate reflected light was obtained by subtracting two independent data sets. In the calculation of these differences, a small mismatch in the recorded scattering angles was observed. This mismatch is believed to have produced a systematic error that is responsible for these discrepancies at the larger scattering angles.

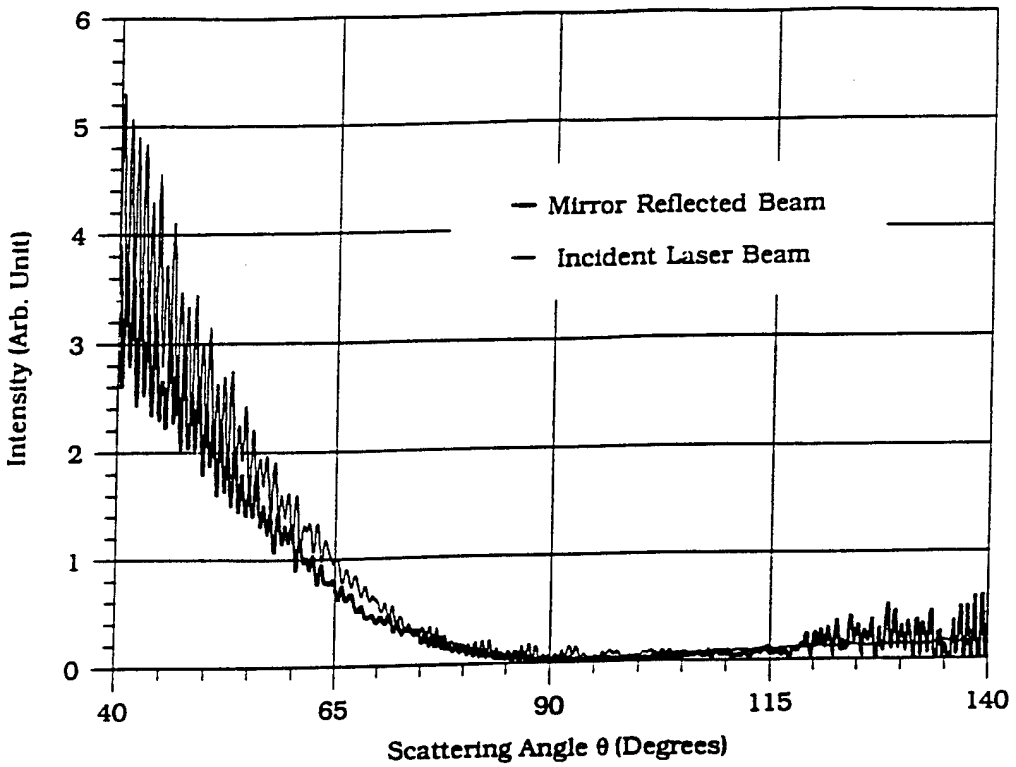

Figure 3. The scattered intensity distribution for the incident laser and for the reflection by a normal mirror. Fiber radius is 19.8 μm, wavelength is 514.5 nm, and polarization is perpendicular to the fiber axis and parallel to the plane of incidence.

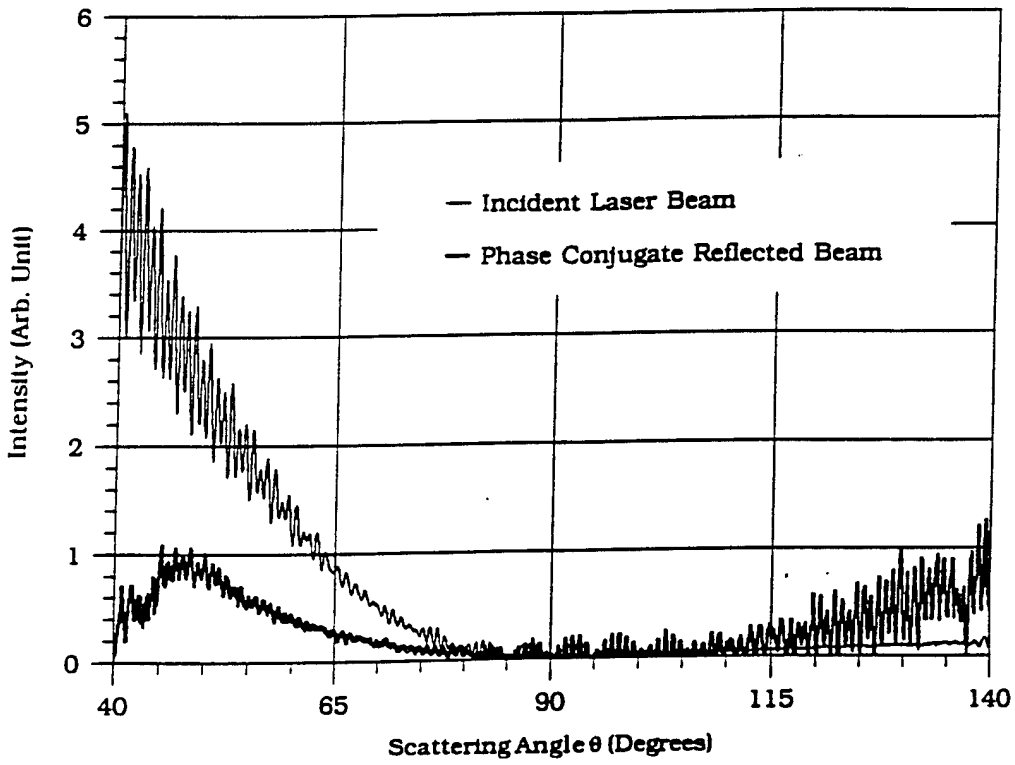

Figure 4. The scattered intensity distribution for the incident laser and for a phase conjugate reflection. Fiber radius is 19.8 μm, wavelength is 514.5 nm, and polarization is perpendicular to the fiber axis and parallel to the plane of incidence.

Next, the conventional mirror is replaced by a $BaTiO_3$ crystal, as in Figure 2. The forward scattered light is collected by a lens placed in front of the crystal. The position of the lens is adjusted so that the forward scattered light within a full cone angle of about 10° is incident on the front face of the crystal. This light together with the incident laser beam is then self phase-conjugated in the $BaTiO_3$ crystal. The phase conjugation of forward scattered light is confirmed by checking that the diffraction pattern of the fiber at detector 1 is the same as the pattern produced by the original beam at detector 2. The angular distribution of the total intensity scattered by the fiber is then measured. As before, the scattered intensity distribution due to the phase conjugate reflected light is determined by subtracting the angular distribution of the scattered intensity without the retroreflection from that observed with the phase conjugate reflector in place. In order to normalize this difference to the signal due to the normal mirror, it was multiplied by the signal observed at detector 1 with a normal mirror reflector and divided by the signal observed at detector 1 with a phase conjugate reflector. Figure 4 shows the intensity distributions for scattering from the incident laser beam and from the phase conjugate reflection.

The structure of the angular distribution produced by the scattering of phase conjugate reflected light is significantly different from that produced by the scattering of light reflected by a normal mirror. In particular, note the suppression of scattering at small angles. However, the anomalous oscillations observed at the larger angles in the last experiment are also present here. Again, this is believed to be a systematic error arising in the subtraction process.

3.1.1.4 Experimental Results: Chopper Based

This systematic error was eliminated, and the data subtraction procedure was avoided in a second set of experiments. In these, the effects due to the scattering of retroreflected light were separated from those due to the scattering of the incident laser beam by placing a mechanical chopper in front of the retroreflector. This chopper modulates the intensity of the retroreflected light and thereby produces a modulation in the intensity of the scattering from the retroreflected beam. The PMT signal due to the intensity of the scattered light is amplified using a lock-in amplifier synchronized to the chopper frequency. These additional components are indicated by dashed lines in Figures 1 and 2. As before, signals due to scattering from the incident beam are obtained in the absence of a retroreflected beam, but in this second set of measurements, the signals due to scattering from the retroreflected beam are given directly by the lock-in output. First, a normal mirror is used to retroreflect the incident beam and the scattered light. The chopper is turned on and the angular

scattering function of the mirror reflected light is measured. In order to provide a calibration for the lock-in output, these data are matched to the data for the mirror reflected light in Figure 3 and a calibration factor is obtained. Results for the intensity distributions of the scattering from the incident laser beam and from the beam produced by reflection from a normal mirror are shown in Figure 5. These data are analogous to those in Figure 3. As expected, the scattering of mirror reflected light shows structure similar to that of the incident laser beam. Note that the anomalously large scattering that appears at large values of θ in Figures 3 and 4 is absent here. Specifically, when using the lock-in technique there is no need to take the difference between two independent data sets, and this introduction of uncertainty in the data is absent. Also, note that due to the long time constant of the lock-in amplifier some of the detailed structure is partially suppressed.

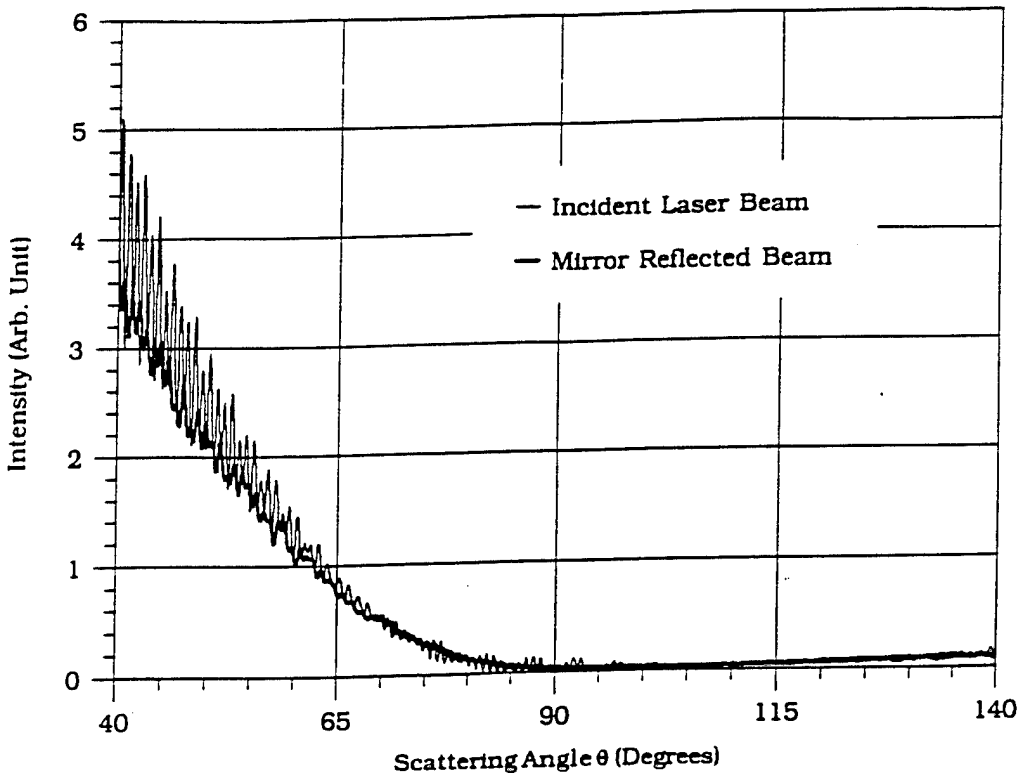

Figure 5. The scattered intensity distribution for the incident laser and for the reflection by a normal mirror. The latter is measured using the chopper and the lock-in (Fig. 1). Fiber radius is 19.8 μm, wavelength is 514.5 nm, and polarization is perpendicular to the fiber axis and parallel to the plane of incidence.

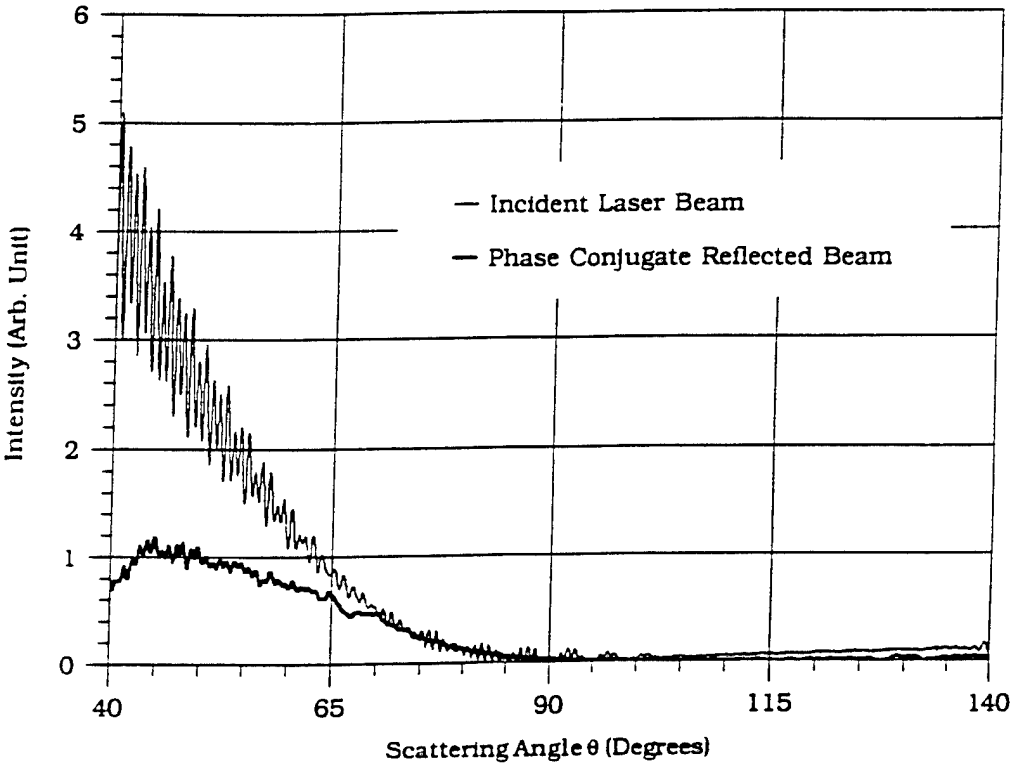

Figure 6. The scattered intensity distribution for the incident laser and for a phase conjugate reflection. The latter is measured using the chopper and the lock-in (Fig. 2). Fiber radius is 19.8 μm, wavelength is 514.5 nm, and polarization is perpendicular to the fiber axis and parallel to the plane of incidence.

Next, the normal mirror is replaced by a $BaTiO_3$ crystal. As in the first set of experiments, the forward scattered light is collected by a lens placed in front of the crystal. The position of the lens is again adjusted so that forward scattered light within a full cone angle of ≈10° is incident on the front face of the crystal. The mechanical chopper is placed between the lens and the crystal as shown in Figure 2. The chopper apertures are large enough to allow a full 10° cone of forward scattered light to pass through them. The chopper is turned on and the angular scattering function of the phase conjugate reflected light is then measured. In order to normalize to the signal due to a normal mirror, the lock-in signal is multiplied by the calibration constant (as in Figure 5) and by the ratio of the signals at detector 1 due to the mirror and conjugator (as in Figure 4). Results for the intensity distributions of the scattering from the incident laser beam and from the beam produced by phase conjugate reflection are shown in Figure 6. These data are analogous to those shown in Figure 4. Again, the angular distribution of the scattering from the phase conjugate reflection shows a significantly different structure compared to that from a normal mirror reflection. As in Figure 4, the scattering is suppressed at small angles, but here it is also observed to be suppressed at large scattering angles. As before, the anomalously large scattering observed in Figure 4 at large values of θ is absent here.

3.1.1.5 Summary

A simple physical interpretation of the suppression of the scattering from a phase conjugate beam can be given. When the incident light is scattered by a fiber of radius 19.8 μm, most of the scattered light is confined to a small cone in the forward direction. Thus, phase conjugation of light scattered into the full angle of 10° is enough to simulate an almost ideal situation of phase conjugating all the scattered light. After the interaction between the fiber and the phase conjugated light the incident wave is approximately recovered; hence, the angular distribution of the scattering from the phase conjugated beam is suppressed. In conclusion, we have observed that if forward scattered light is reflected by a phase conjugator, the angular scattering it produces is suppressed relative to that produced upon reflection by a normal mirror. However, quantitative relationships have not yet been obtained.

3.1.2 Dynamic scattering experiments

3.1.2.1 Introduction

The initial dynamic scattering experiments involved the use of a sealed-off cells containing polystyrene microspheres suspended in water, thereby forming a colloidal

suspension. In the experiments that follow, scattering cells of varying interaction length, and containing scattering sites of varying diameters and concentrations, are described. Scattering measurements were made at various locations surrounding the cell, including on-axis and at angular offsets relative to the plane of incidence, as shown in Figure 7. An argon ion laser operating at 514.5 nm was employed as the source, and a self-pumped phase-conjugate mirror using a single crystal of barium titanate created a wavefront-reversed replica of the light transmitted through the cell. A telescope is used to image the scattering cell at its mid-plane into the conjugator. For comparative purposes, a cat's eye retroreflector is employed to realize the non-conjugate wave — non-conjugate, that is, except for the fact that simple tilt errors are corrected by its action.

Based on the various classes of scattering sites discussed in Section 2.1, the present case falls under the category of "highly transparent or translucent, dynamic scattering sites." As such, a key condition for the backward-going beam to reduce off-axis scattering requires that the system spatially resolve only the exterior of the individual scatterers, and not necessarily its internal features. This state of affairs places far less constraints on the optical collection system (or, field of view) relative to the case described in the previous section (the stationary quartz fiber) where all of the detailed internal spatial features of the fiber were necessary to be resolved by the system in order to eliminate the scattering.

The less demanding condition in the present case stems from the fact that the scatterers are, in essence, "frequency tagged" via their Doppler motion. Thus, assuming that the conjugator does not respond fast enough to track these Doppler shifts, local "holes" will form in the real-time gratings within the conjugator, which will correspond to apparent "shadows" left behind by the scatterers — which will be burned into the wavefront-reversed replica. The conjugate wave will then retraverse its incident path, reproducing the shadows, thereby avoiding the scattering sites as it propagates through the medium. Thus, the requirements for this system to function are that the conjugate system need only spatially resolve the global features of the individual sites as well as any slowly varying drifts. In this way, the "holes" left by the Doppler-shifted scattering sites will be tracked by the backward-going beam in real time, leading to a reduction in the scattering experienced by the backward-going beam.

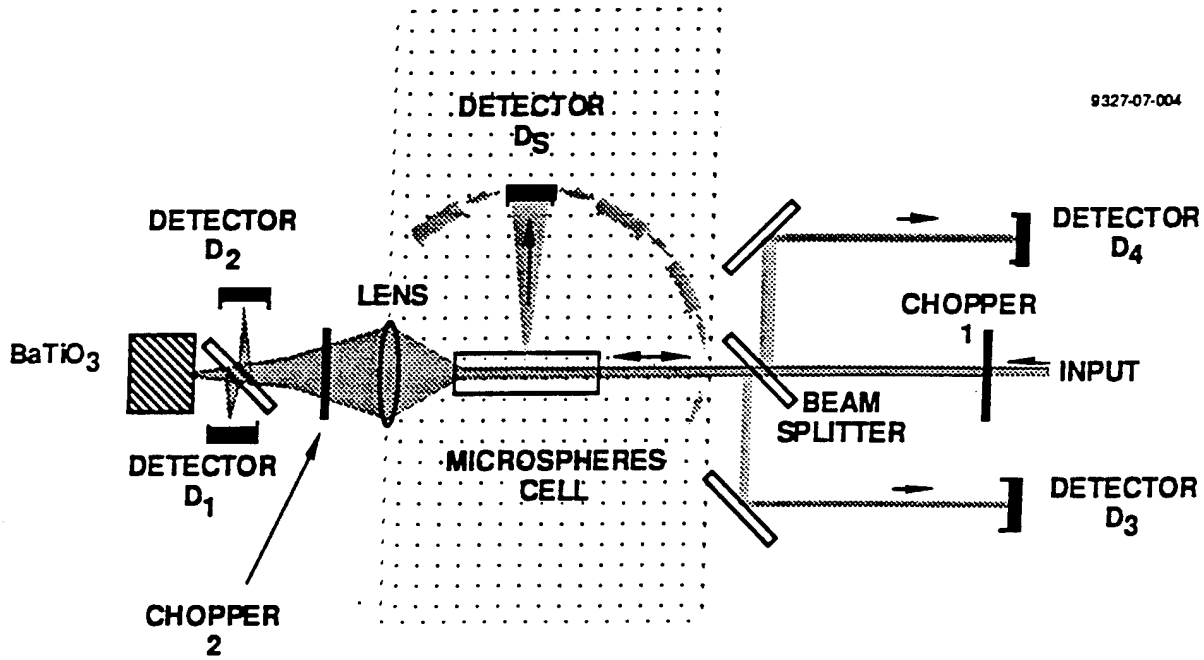

Figure 1. Basic experimental configuration.

A self-pumped barium titanate conjugator is used to generate wavefront-reversed replicas of an incident, scattered beam. For comparative purposes, a cat's eye retroreflector is positioned in place of the conjugator. Detector D_S monitors the wide-angle scattered beam.

The scattering test cell contains various mixtures of single-sized polystyrene spheres (with nominal diameters of 50 μm, 5.0 μm, and 0.5 μm), as well as mixed-sized suspensions. The size variability was chosen so that the optical system could either completely resolve, barely resolve, or not resolve the scattering sites, respectively. An Air Force resolution chart in conjunction with a CCD-based video processor was used to quantify the minimum resolution of the system. Care is taken to minimize background scattering, and to reproduce scattering cell parameters as well as we can, given the complex interaction between settling time of the scattering sites, swirling effects during cell agitation, and a fairly long conjugate signal buildup time. In order to discriminate against noise sources, mechanical choppers are used to frequency tag the forward and backward components of the scattered light.

Using this system, our preliminary results indicate that the wide-angle scattering of the conjugate wave by the colloidal suspension can be reduced by more than a factor of two relative to that of the retro-reflected reference beam. For these initial measurements, the scattered light was measured along the direction of the polarization vector of the incident beam. On-axis transmission of the conjugate wave through the scattering cell was, in one cell, increased by almost 50% over that of the cat's eye reflected beam. We speculate that these photons can be attributed to the ballistic and/or snake-like components,[5] which, in essence, avoid, or "miss," the scattering sites through passage in the scattering medium.

In these experiments, each sealed-off cell is filled so that no air/water interface is present internal to the cell, and both the laser and conjugator are mounted on a stable optical table. However, in many real-world scenarios, platform movement and dynamic water-wave motion can seriously impact the maintenance of a phase conjugate link. As we discuss in Section 4, it is for these reasons that we recommend as a future task to augment the phase-conjugate mirror with a tilt compensation apparatus, so that the forward-going beam remains bore-sighted to the conjugator under platform movement and surface turbulence conditions and then repeat the basic set of measurements that was performed on the current program. In addition, by introducing an air/water interface, the additional benefit of the autotracking property of phase-conjugate beams can be evaluated under more realistic conditions, including surface-wave motion and turbulence.

The experiments were designed to measure the temporal and spatial scattering produced as a function of angle and polarization. Because this program was applicable to coherent communication or direct image transmission, there was a particular interest in scattering produced in the forward and backward directions. We also investigated the scattering as a function of the dimension of the microspheres.

This was motivated by the variation of the naturally occurring scattering centers in sea water. Therefore we chose the diameter of the microsphere's to represent a range of values varying from much greater than the wavelength of light propagating through the suspension, to ones which were comparable to the wavelength of light.

We were motivated to reduce scatter from suspended particles in order to develop techniques for coherent communication or direct image transmission. Various techniques have been demonstrated in the past with varying degrees of success for overcome scattering losses. These approaches included using synchronous scanning in conjunction with a reduced field of view in order to minimize the received back scatter. Another method uses incoherent communication employing a wide acceptance angle and an extremely narrow spectral band filter, such as an atomic resonance filter (of the "Marling" variety or a resonant Zeeman or Stark-induced birefringence class of filter).

We have chosen to capitalize on the properties of phase conjugation in order to reduce scattering. There has been previous work which produced evidence of reduced scattering using phase conjugation. This work includes the lensless imaging concept first proposed and demonstrated by Levenson.[10] In these experiments a photoresist mask was projected through a beam splitter onto a phase conjugate mirror. The phase conjugate image produced is reflected by the beam splitter and directed onto a substrate plane. Because the fidelity of the phase conjugate image is extremely high, the image formed on the substrate can have very high spatial resolution. The relationship to the present scattering experiments becomes more apparent if the features of the transmission mask are divided into two regions: the transmitting portion and the adjacent opaque regions. In the lensless imaging experiments, the conjugate beam reconstructed all of the mask features; that is, the transmitting portion consisted of both bright and opaque, or dark, regions. Therefore, in essence the conjugate image reproduced not only the bright regions but also the "shadows." Therefore, even If the mask features are comparable to, or greater than, the wavelength of light, then the result of the light propagating through the mask is similar to the forward scattering produced by suspended particles. Our experiment can be viewed in this context as a "distributed" mask.

If all of the light scattered from a particle in the forward direction can be collected and focused into a phase conjugate mirror, the complete phase conjugate beam will be produced. The conjugate beam produced will then retraverse the media (in the backward direction) and form the electromagnetic field originally produced at the scattering particle. If the beam perfectly reconstructs the field at the particle, the scattering produced in the backward direction by the particle will be a minimum. If not all of the scattered light is collected then the fidelity of the conjugate beam will be degraded. Yet, so long as the system can resolve the features of the opaque regions,

then the scattering will be reduced, with an "approximate" wavefront-reversed replica emerging from the system on the backward-going pass.

In what follows, we first describe our experimental apparatus in some detail. This is followed by three sets of measurements: (1) the measurement of the settling time of the microspheres as a function of microsphere diameter; (2) the determination of the imaging resolution of our apparatus; and (3) the measurement of the scattering versus angle for the various sized microspheres. Knowledge of the settling time of the microspheres is crucial in establishing the maximum length of our experimental data runs — since, once the particles settle out, the scattering measurements become invalid. Similarly, knowledge of the spatial resolution of our system is key in ascertaining the ability of the conjugate beam to faithfully reproduce the "shadow" features left by the scattering of the forward-going beam out of the system — since, if the shadows can't be resolved, then the reduction in scattering will not proceed efficiently.

3.1.2.2 Experimental Apparatus

There were two basic geometries used when the phase conjugate propagation studies were conducted to determine the reduction in scattered light using a wavefront-reversed replica. This first orientation was designed to be representative of communication between two submerged vessels at approximately the same depth. The second set of experiments were designed to simulate communication when one end of the link was on a submerged vessel and the second end of the link was located above the first link on either a submerged platform or a platform above the water.

The scattering produced by sea water can be simulated by polystyrene microspheres suspended in a solution. In order to mimic the scenario of communication at the same level, the cylindrical cell containing the microspheres was oriented so that gravity was acting perpendicular to the direction of the beam propagation. In the second set of experiments, the beam propagated down through an air/water interface in the direction of the gravitational pull.

A schematic of the first experimental apparatus is shown in Figure 7. The beam propagates from right to left, originating at the word labeled *INPUT* in the figure. The laser was operating single longitudinal and transverse mode at a wavelength of 514.5 nm. The input beam was modulated by the chopper number 1 at a frequency of about 1 kHz in order differentiate the scattered produced in the same volume from light propagating in the forward direction and that which was produced by light propagating in the backward direction. A lock-in amplifier was used to phase-detect this component, thereby discriminating against other spuriously scattered light from corrupting the measurement. Given the small amount of scattered light to be detected (especially at angles in the 90° range in the case of p-polarized beams), the light from

the cell was imaged onto the detector, with mild spatial filtering and opaque tubes (placed over the detector and optical components) to block unwanted light, thereby defining the angular field-of-view to about 5° in both directions, with minimal background. The first beam splitter (BS1) in conjunction with detector number four are used to monitor in the input beam power.

The beam then propagates through a cell containing the colloidal suspension. The microspheres were made from polystyrene with diameters of 0.5, 5.0 and 50 μm. The concentration of particles was designed to produce single scattering events and therefore the overall transmission was engineered to be greater than 90%. We had available a selection of cell geometries depending upon the particular experiments. Two of the cell designs were cylindrical, 2.5 cm in diameter and either 2.5 cm or 10 cm in the dimension parallel to the beam propagation direction.

We also used a thin rectangular cell 1 cm wide by 3 cm tall and 0.1 cm in the direction of beam propagation. This cell acted as a thin "sheet" of scatterers and served two functions: First, the thickness of the cell could be made comparable to the depth-of-focus of the optical system. In this case, we were assured that our system can spatially resolve the positions of the scattering sites, enabling us to better quantify the scatter reduction performance of the phase-conjugate wave. A second reason for using such a thin sheet of scattering sites is that one can flow the scattering sites through the cell (an auxiliary water pump was used for this purpose). This setup enabled us to image the scattering sites as they flowed through the cell with a CCD camera, and to therefore experimentally establish that, indeed, the conjugator was responding fast enough to "track" the motion of the scattering sites. We were also able to vary the velocity of the particles in the direction transverse to the beam propagation direction with this system. The particle velocity could be maintained between 0 and 600 μm/sec via regulation of the flow rate.

A goniometer was set up to measure the angular scattering component of the light by the various test cells. A detector D_S was used to detected the light which was scattered by the particles. The detector was mounted on a circular track, centered at the center of the microsphere cell. The angular position of the detector on the track was referenced with respect to the beam propagation direction and calibrated in degrees. In order to improve the signal to noise ratio, a 10 cm focal length lens was used to image the central volume of the cell onto the detector. By placing the lens 2f equidistant between the cell and the detector a 1:1 magnification was obtained and the (undesired) scattered light produced outside the imaged volume was significantly reduced.

A collecting lens was used to focus the light emerging from the cell into the phase conjugate mirror. This imaging lens was f/# 2.4 and enabled us to resolve 3 μm features. Detector D_2 was used to monitor the light transmitted through the cell and

incident on the phase conjugate mirror. In order to improve the signal to noise ratio, the output from this detector was fed into a lock-in amplifier tuned to the frequency of chopper 1. This also allowed us to separate the contribution to the scattered light produced by the forward and backward (phase conjugate) propagating beams

The phase conjugate mirror was realized by using the self-pumped geometry in a photorefractive crystal, called the "cat" configuration.[9] This nonlinear material consists of a single crystal of poled photorefractive $BaTiO_3$. P-polarized light was used to couple into the optimum r_{42} electro optic coefficient. The phase conjugate reflectivity with this crystal was in the range of 40-60%. For these experiments, an optical input laser intensity at the conjugator of approximately 0.8 W/cm^2 was used.

The phase conjugate beam generated would retraverse the original input beam path. A portion of the conjugate light was reflected by the beam splitter 2 into detector D_1. This allowed us to monitor the conjugate light entering the microspheres cell.

The majority of the light was transmitted through the beam splitter and was modulated by the chopper number 2 at a frequency (in the range of 5 kHz) which differed from that of the other mechanical chopper. The use of a pair of choppers that sandwiched the cell allowed us to differentiate the scatter produced by the phase-conjugate beam in the same volume of the cell from light propagating in the forward direction. The light then retraversed through the collecting lens and into the cell containing the microspheres. By employing a pair of lock-in amplifiers, simultaneous measurements of the forward and backward scattered light can be made for real-time calibration purposes, so that systematic effects of particle settling, for example, can be normalized out.

3.1.2.3 Off-Axis Scatter vs. Settling Time

As we discussed above, knowledge of the settling time of the microspheres is crucial in establishing the maximum length of our experimental data runs — since, once the particles settle out, the scattering measurements become invalid. Therefore, we set out to experimentally measure the scattering time for each scattering candidate we evaluated. This measurement, therefore determined the maximum time that data can be taken for a given run. Of course, this time must be much greater than the phase-conjugate build-up time, otherwise, the conjugate wave will not be capable of "tracking" the scattering centers as they settle out due to, for example, gravitational effects. In other words, the amount of transverse settling during the phase-conjugate response time (and round trip photon transit time) must be much less than the diameter of the scattering site — assuming, of course, that the optical system can spatially resolve the particle. This latter point is discussed in the next subsection.

Depending upon the microspheres size, the particles will stay in solution for different lengths of time because of the action of gravity and viscosity. The largest and

heaviest particles will precipitate out first while the smallest particles will be kept in suspension the longest due to the effects of Brownian motion. This data for these measurements are shown in the graph of Figure 8. In this figure, the transmission in per cent at a single wavelength (514.5 nm) is plotted as a function of time in minutes for the various microsphere diameters. Prior to making the measurements the respective cells were agitated for 0.5 minutes (30 sec).

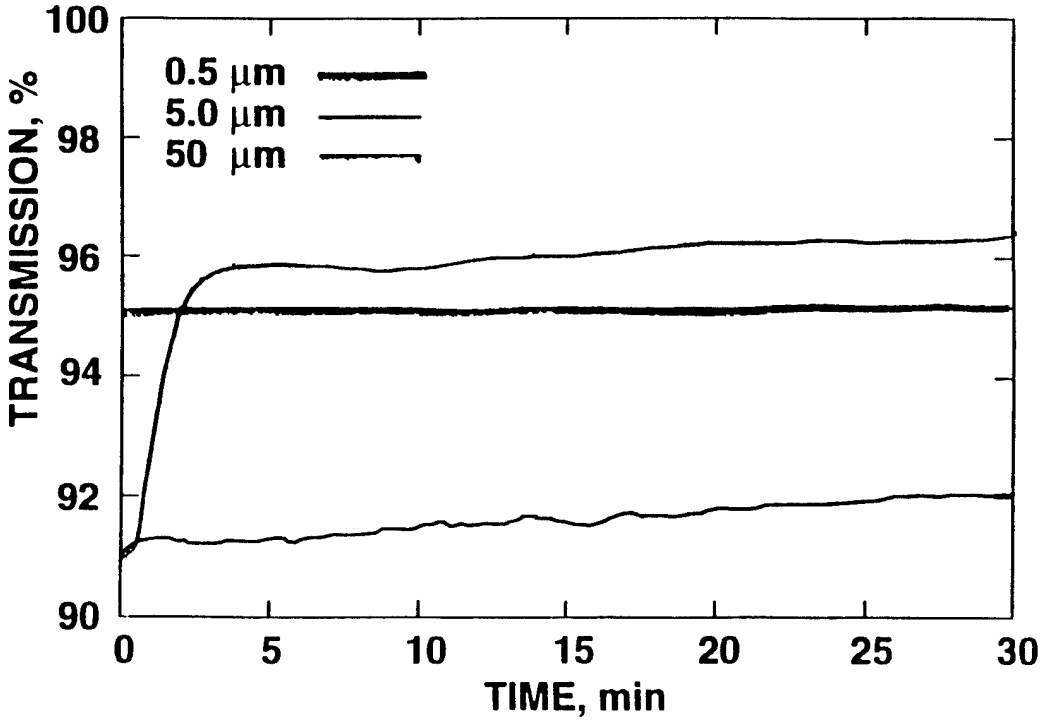

Figure 8.
Plot of settling time for three different-sized microspheres.

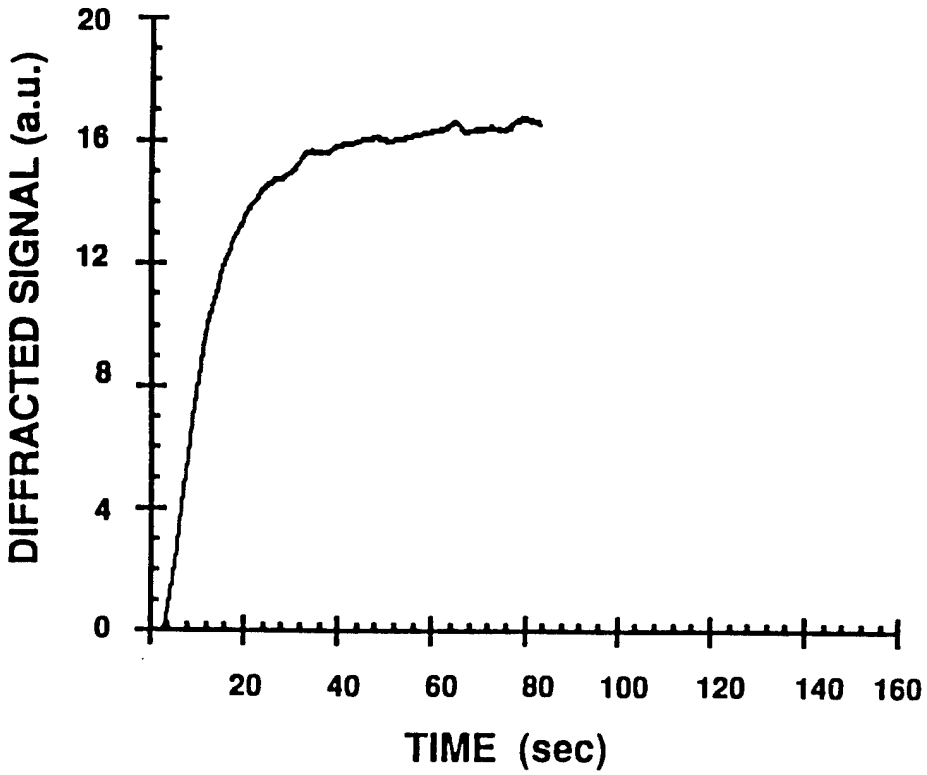

Figure 9.
Measured phase-conjugate build-up time for a crystal of barium titanate.

The initial transmission for each run differs slightly owing to the concentration of the microspheres for the given diameter. As discussed earlier, attempts were made to have each cell transmit a large fraction of the incident beam so as to minimize the possibility of multiple scattering sites, so that multiple-shadowing effects are small relative to single-shadowing events. One can see that the transmission for the 0.5 μm diameter microsphere cell is essentially constant over the 30 minute interval, indicating very little settling, if any for this case. On the other hand, in the case of the 5.0 μm microsphere solution, the transmission is seen to increase by ≈1 % over the same time interval as the particles settle out of solution. The change in transmission is the most dramatic for the 50 μm particles. In this case, one can see that there is almost a 5% increase in transmission in the first two minutes alone.

The results of these experiments indicate that there is an explicit time dependence for the scattering measurements to be made using different size microspheres in order for the experimental run to be most easily interpreted. We therefore parameterized our scattering measurements not only by the size of the microspheres, but additionally, by the length of time of the given measurement.

For comparison of the relative time scales, we show in Figure 9 the measured phase-conjugate build-up time for our experimental parameters. Recall, that the intensity incident on the conjugator was about 0.8 W/cm^2, which is consistent with the measured build-up time of about 2 to 4 seconds. Based on this measurement, coupled with the settling time measurements above, the experiments conducted on the cells under the force of gravitationally induced settling appear to be valid, in terms of establishing the ability of scatter reduction with a reasonable degree of confidence.

As an additional experimental tool, we built and designed a thin vertical cell that could counteract the effects of gravity by flowing the microsphere solution upwards slightly. The cell was connected to a pump which recirculated the solution. The velocity could be accurately controlled by varying the pump rate. The velocity of the particles could be controlled between 0 to 600 μm/sec. By selecting the correct velocity for each particle size the effects of gravity could be counteracted. This same thin-cell system was used for the resolution studies and imaging experiments described next.

3.1.2.4 Imaging of Scattering Centers

The same thin-cell pump apparatus used to counteract the settling effects of the microspheres (mentioned above) was also used for several different image calibration experiments, including spatial resolution and phase-conjugate tracking. In the former case, knowledge of the spatial resolution of our system is key in ascertaining the

ability of the conjugate beam to faithfully reproduce the "shadow" features left by the scattering of the forward-going beam out of the system — since, if the shadows can't be resolved, then the reduction in scattering will not proceed efficiently. Secondly, the ability of the phase-conjugate beam to image the flowing microspheres in real-time (without deblurring) experimentally establishes the possibility of the system to reduce scattering of the sites. Conversely, when deblurring does occur (due to conjugator response-time limitations), then one expects that the scattering reduction capability of the conjugate wave to degrade.

In Figures 10, 11 and 12, we show results on both of these experiments. Figures 10 and 11 show results of a phase-conjugate lensless imaging experiment using an Air Force resolution chart as the test object. In this experiment, the resolution chart was illuminated by a spatially filtered probe beam and directed onto the phase-conjugate mirror. The phase-conjugate return was picked off by a beam splitter, directed onto a CCD camera and processed using an in-house video frame grabber and level slicer. The raw conjugate image is shown in Figure 10, whereas a level sliced trace across the chart is shown in Figure 11. From this data, it was determined that the conjugator/lens resolution limit was ≈ 3 μm; in a separate measurement, the image system resolution was determined to be ≈ 12 μm.

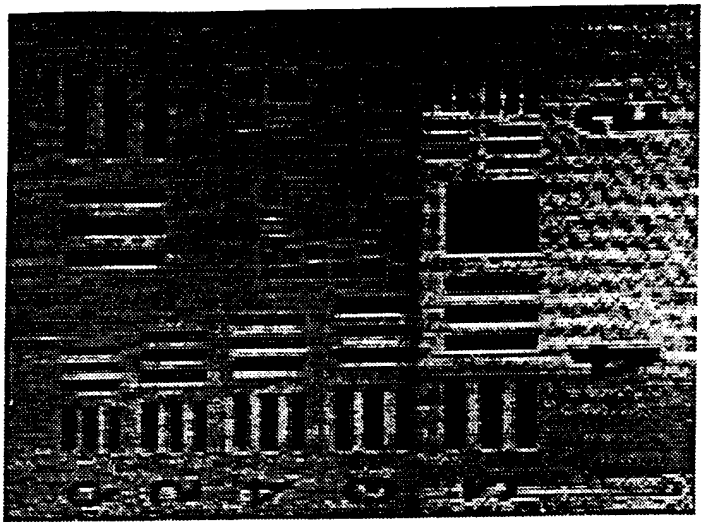

Figure 10.
Phase-conjugate lenless imaging experiment using an Air Force resolution chart.

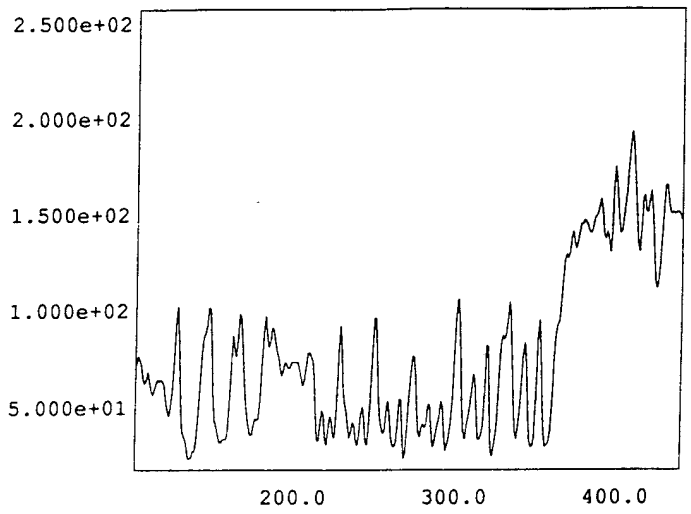

Figure 11.
Video-processed section of Figure 10 showing the edges of the lenless image chart.

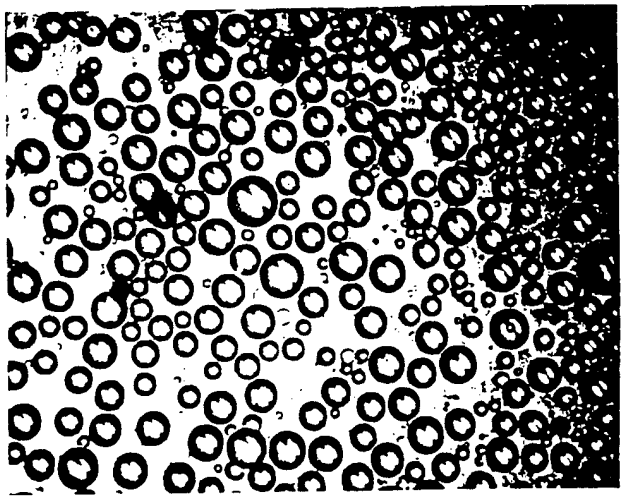

Figure 12.
Frame-grabbed video CCD image of a phase-conjugate image of a microsphere ensemble.

We also performed real-time imaging experiments using the flowing cell with various sized-microspheres. Using this apparatus, a phase-conjugate, lensless imaging experiment was performed using the same geometry as described above for the case of the resolution chart. A typical example is shown in Figure 12, where an image is shown of the microspheres, which was captured by the video frame grabber system and magnified for ease of viewing. Note that the shadows appear with high spatial resolution (across a relatively flat field) due to the light scattered out from the optical acceptance angle. Note also, that the system can resolve the microspheres, as distributed throughout the thickness of the cell (i.e., along the optic axis of the system). With this apparatus, we also determined that the conjugator can, indeed, track the flowing microspheres at flow rates consistent with those of the settling time for the respective diameters, as shown in Figure 8. This was accomplished by varying the flow rate and viewing the reconstructed conjugate image over the range of scale times, typical of the measured settling times above.

3.1.2.5 Off-Axis Scatter versus Particle Size

A key experimental measurement on this effort was to quantify the scattering of a conjugate wave relative to that of a nonconjugate wave. Given the calibration data as measured in the above series of preliminary experiments, we established confidence in the data regarding scattering effects which we claim to be of interest for various systems applications described in the previous sections. On this subtask, we performed a series of experiments designed to demonstrate the ability of phase conjugation to reduce the scatter produced by microspheres in solution.

For a transmitting media, the off-axis scatter can be defined as the ratio of the scattered power per unit solid angle normalized to the incident power. In the measurements that follow, we employed the basic experimental apparatus sketched in Figure 7 above. Using this setup, we measured the off-axis scatter as a function of the angle, as defined by detector location, the center of the cell, and the optic axis — all parameterized by the microsphere size. The polarization of the input light was s-polarized; we also made measurements using p-polarization . The detector D_S was the moved in an arc which was perpendicular to the plane of incidence.

For this experimental run discussed below, we oriented the cell in a vertical direction, so that the scattering sites were always uniformly in the beam path as they settled. The goniometer was oriented so that the off-axis scattering of the respective beams can be measured, ranging from their respective forward-going direction (defined as zero degrees), in 5° steps, to their respective backward-going scattering direction (defined as 180°). The polarization vector of the incident laser beam for the

data below was set so that it was aligned perpendicular to the plane containing the scattering angles, thereby not systematically affecting the scattering as a function of angle.

We made relative measurements because we were interested in a study which compared the effectiveness of a true phase conjugate mirror with that of a pseudo conjugate mirror. The pseudo-conjugator was in the form of a cat's eye reflector, consisting of a lens with a 100% reflector at the rear focal plane. This element enabled the return beam to compensate for beam wander and tilt errors. Given the high degree of reflectivity of this element, a means by which the conjugate wave can be normalized is established by taking the ratio to the two beams at each angular setting of the goniometer.

The ratio of the off-axis scatter was computed in the following manner. The detector D_4 was used to monitor the total incident power of the forward beam propagating into the cell. A conventional mirror would be inserted, one focal length from the collecting lens (downstream of the cell) in order to form the pseudo conjugator as discussed above. Because the reflectivity of the mirror was 100% the light reflected back into the cell could be used to establish a baseline for the power of the backward propagating beam incident on the cell. This power was monitored by the detector D_1. Monitoring this power allowed us to normalize the signal detected by detector D_S to the intensity of the backward propagating beam.

In Figures 13, 14, and 15, the results of our detailed scattering measurements are shown, where the angular dependence of the scattering is plotted as a function of angle for both the conjugate wave and for the retro-returned beam. The respective plots are given for the three microsphere diameters employed in our measurements: 0.5 μm, 5.0 μm, and 50 μm. As discussed above, in each case, the concentration of the microspheres was adjusted to yield approximately 90% transmission of the incident laser beam through the 10 cm long cells. The cell length was chosen to be long enough as to enable our measurements to function over a large angular range (centered at the cell mid-plane), thereby avoiding reflections from the cell end-caps. On the other hand, this length "stressed" the optical system to spatially resolve the microspheres along the entire interaction path length. The cells were vertically oriented for these experiments, with the incident probe beam directed in a downwards path from above the cell. The data was obtained by recording the power detected by detector D_S (as normalized to that detected by the ratio of detector D_2 to D_4) and measured as a function of angle for a given particle size, thereby yielding the desired scattering flux. It is clearly seen that, in every case, and for all measured angles, the conjugate wave experiences less angular scattering than that of the nonconjugate wave. The dispersion of data is due to microsphere settling in the cells for the various runs, which was most pronounced for the 50 μm diameter polystyrene case.

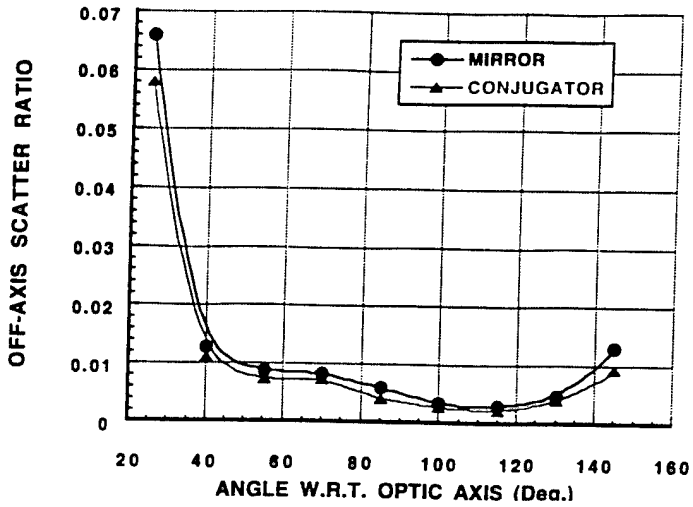

Figure 13.

Plot of angular scattering flux for a phase conjugate and a retroreflected beam for a cell containing 0.5 μm microspheres.

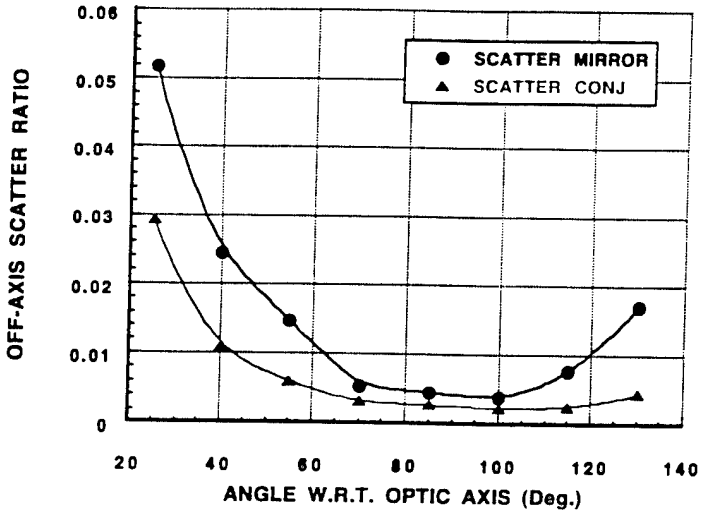

Figure 14.

Plot of angular scattering flux for a phase conjugate and a retroreflected beam for a cell containing 5.0 μm microspheres.

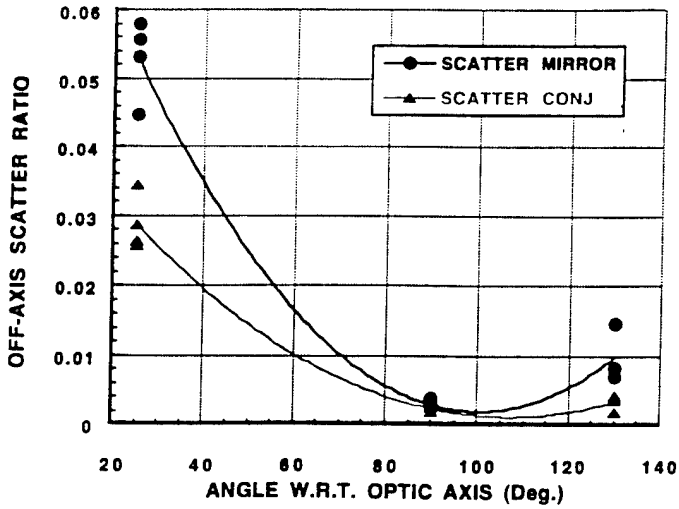

Figure 15.

Plot of angular scattering flux for a phase conjugate and a retroreflected beam for a cell containing 50.0 μm microspheres.

In Figure 16, we show a plot of a composite result of all scatter reduction results for the three different particle sizes employed in our experiments, and for several different data runs. It is seen that the reduction in the scattering using a conjugate wave is on the order of a factor two relative to a nonconjugate beam in the case of particle sizes that the system can resolve. Furthermore, even below the resolution limit of the system, this enhancement ratio is ≈ 40%, still in favor of the conjugate wave. For this plot, the scatter reduction ratio was taken for data given in Figures 13, 14, and 15, at an angle of 25°.

In another set of experiments, we measured the enhancement in the transmission of a conjugate wave relative to a nonconjugate wave. For these runs, we employed a thin cell of 1 mm in length, so that optical system could resolve the interaction region throughout its path length. The results of this set of measurements is shown in Figure 17. From the figure, we see that the increase in transmission is approximately 10% when the system can spatially resolve the scattering sites. Perhaps another way to quantify the data, as is also shown in the figure, is to plot the "scatter compensation" relative to the nonconjugate wave. In this representation, we see that since the initial transmission loss was set to ≈10%, most of the scattering incurred by the forward-going probe wave are not present by using a phase-conjugate mirror. Since we are comparing relatively small numbers (the cell concentration of scatterers was held to a low amount), there is a relatively large dispersion in the data. In any case, this metric demonstrates the utility of employing a conjugate device in a communication systems application.

In our experiment, we obtained the enhancement ratio by comparing the transmission of the respective backward-going waves through the cell in both cases. This measurement, in essence, represents the net increase in the conjugate-wave efficiency, which could, in principle, be also obtained (with much difficulty!) by integrated the decrease in scattering losses over all angles experienced by the conjugate wave. We chose to determine this figure of merit by taking the ratio of the detector D_3 level to that of the incident phase conjugate return, as measured by detector D_1. Moreover, not shown here, but evident from qualitative observations of the beams in our apparatus, the conjugate wave emerged as a relatively "clean" plane wave, whereas the nonconjugate wave emerged as a rather distorted beam, as seen by placing a card in the path of detector D_3 and visually observing the two beams.

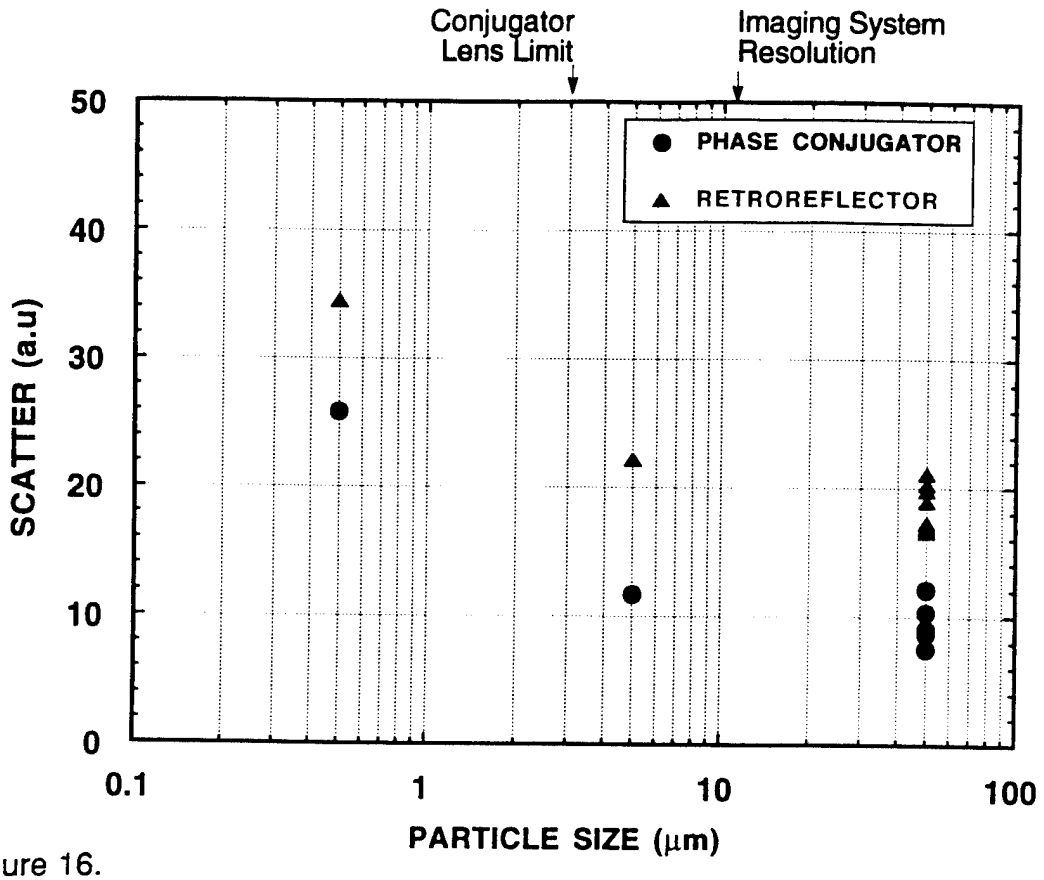

Figure 16.

Composite plot of normalized scatter reduction through a dynamic scattering cell as a function of microsphere diameter.

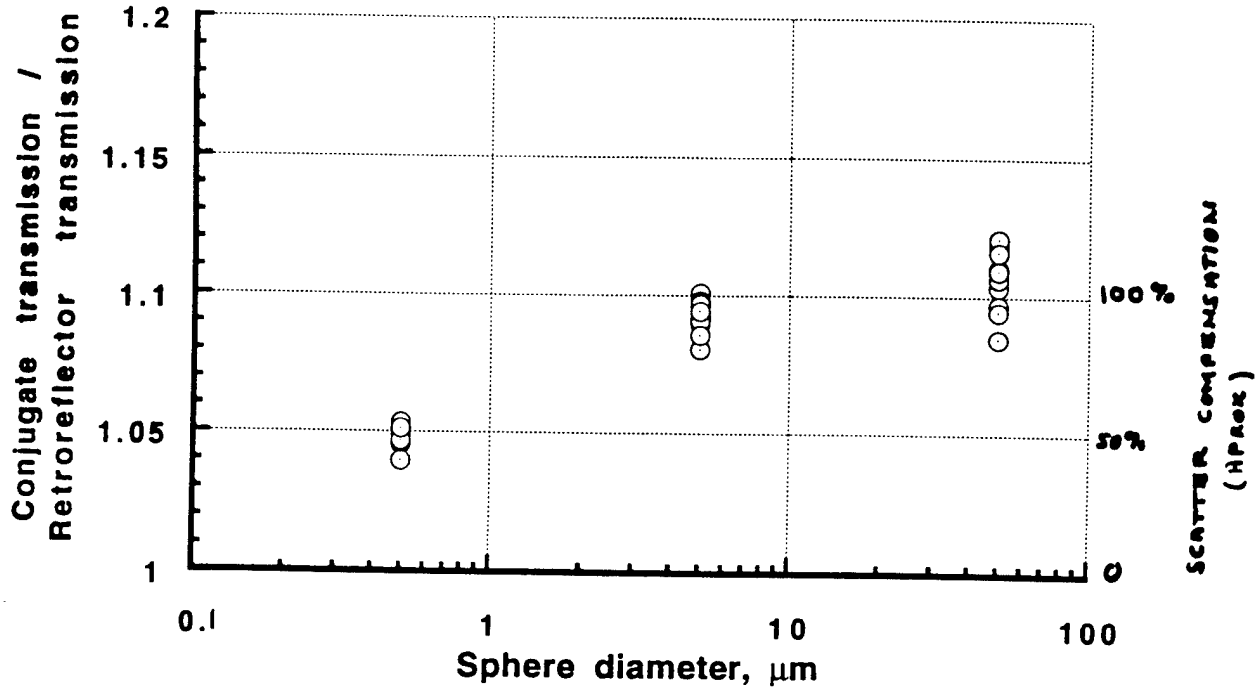

Figure 17.

Composite plot of normalized enhanced transmission through a dynamic scattering cell as a function of microsphere diameter. Also shown is the recovery ratio of the same set of data.

3.1.2.6 Summary

In conclusion, we have observed an enhancement approaching 100% in the transmission of a conjugate wave through a dynamically scattering medium relative to that of a retro-reflected beam. The scattering versus angle of the beams through the cell was also measured using a goniometer for three different microsphere diameters, with the result that, for all angles measured, the conjugate wave experienced less scattering with an average improvement (i.e., less scattering) on the order of two, again relative to a nonconjugate wave. Moreover, the spatial quality of the conjugate wave was superior to that of a nonconjugate wave after traversing the scattering medium. These results were obtained for scattering sites that can be spatially resolved by the conjugator and associated optics; even for small scatterers (below the resolution limit) an enhancement was also measured.

3.2 Remote Sensor System

3.2.1 Introduction

Based on our experience with adaptive optical systems, a lidar system to sense global speed of a collection of scattering sites should see a major improvement in system performance when augmented with a phase-conjugator. Improvements may arise from a number of effects, including the coherent return of the detected signal, compensation of differential Doppler shifts within the ensemble, as well as minimal off-axis scattering of the interrogation beam. In order to ascertain the merits envisioned, we employed the basic experimental apparatus used on the previous task, including the $BaTiO_3$ self-pumped conjugator, collection optics, and probe-beam parameters. Various test cells were configured with host fluids and scattering sites whose length and time scales "matched" those of the spatial and temporal response of the existing conjugator and the optical system. The ability of the conjugator to minimize off-axis scattering, rephase the collected receive beam, and to extract a global modulation test signal from a spatially and spectrally noisy background can then be evaluated under reproducible conditions on a laboratory testbed. These experiments were performed within the Optical Physics Laboratory at Hughes Research Laboratories by G.J. Dunning, M.L. Minden, and D.M. Pepper.

3.2.2 Experimental Apparatus

The basic system architecture employed for the proof-of-concept demonstration of the approach is illustrated in Figure 18. An argon ion laser at 514.5 nm is used as the source. The laser output beam is directed at a scattering cell, with the light

scattered at 90° collected by a relatively fast optical system (f/1.2) and relayed to the self-pumped phase-conjugate mirror. The conjugated light retraces its path and is picked off by a beam splitter placed upstream of the scattering cell. The received light is then directed into a single-mode, polarization-preserving, four-port optical fiber pigtail coupler. A second beam, the local oscillator, is coupled into the second input port of the fiber coupler, where it is combined with the probe beam. This second beam forms the coherent local oscillator beam, which is derived via beam-splitting off a portion of the input laser beam upstream of the experimental apparatus. Since the conjugate beam at this point in the optical system has its initial wavefront essentially restored, it is basically in the form of a "clean" plane wave, enabling relatively high-efficiency coupling into the fiber coupler. The coherent oscillator beam first passes through a 40 MHz acousto-optic modulator prior to entering the fiber pigtail, thereby establishing a heterodyne detection capability. A high-speed photodetector is employed at the third port of the fiber coupler and its electrical output is directed into an rf spectrum analyzer for signal analysis. The fourth fiber-coupler port — which can be employed in the case of a common-mode detection system — was not used for these measurements, since the signal-to-noise was sufficient for this evaluation.

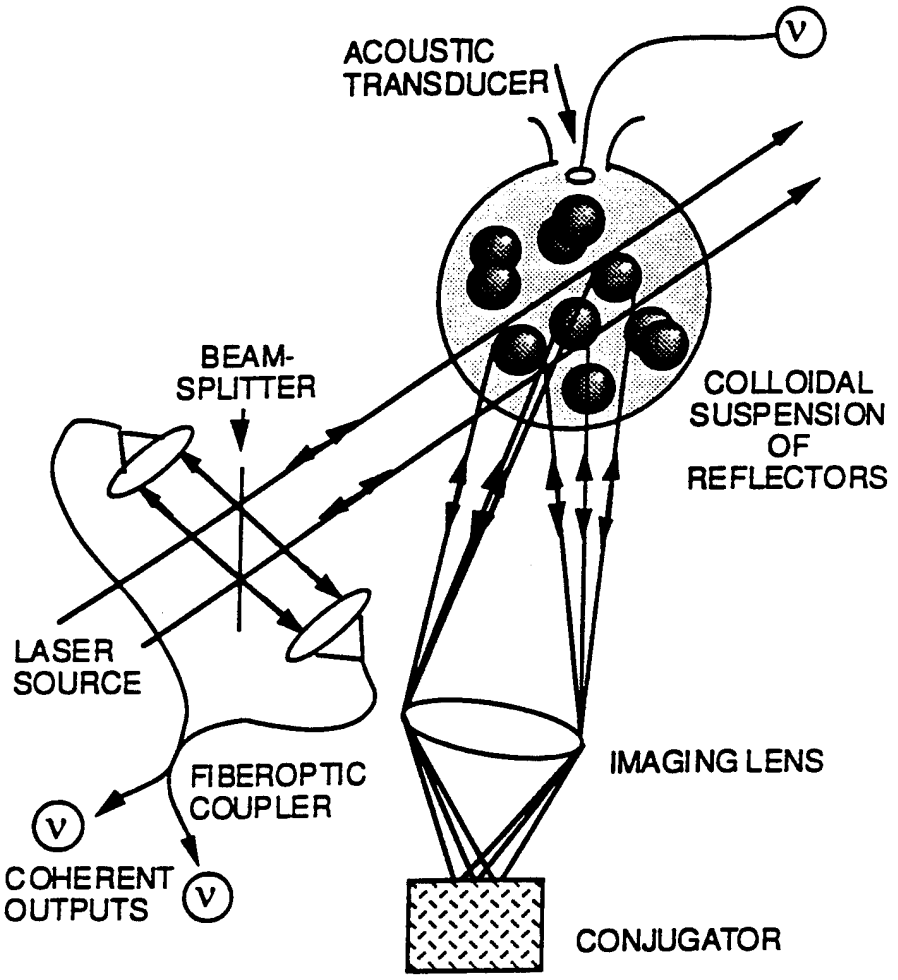

Figure 8. Remote Sensor Demonstration. A probe beam interrogates a suspension of scattering sites, which undergo simultaneous global motion and random, differential motion. A self-pumped conjugator compensates for the differential phase shifts, while preserving the overall phase motion of the ensemble. The resultant double-passed beam reforms constructively at the receiver which, in this case, consists of a fiber-coupled beam combiner.

Controlled global phase shifts could be introduced via an acoustic transducer immersed into the suspension or attached directly to the cell walls. The ability of the lidar system to detect the global transducer signal is determined by coherently mixing the phase conjugate return with a sample of the probe wave, and looking for a spectral component at the transducer's drive frequency. In our experiments, we attached a PZT transducer to the scattering cell wall, which gave rise to global motion of the scattering sites, in addition to the inherent differential motion. The PZT was operated at frequencies ranging from 20 kHz to 1 MHz, with drive voltages in the range of 5 volts to 20 volts. The resultant displacement of the scattering spheres was estimated to be in the range from 5 nm to 50 nm. This perturbation, which can be viewed as a phase-modulation encoding of the optical probe beam upon double-passing the scattering site ensemble, appeared as sidebands in the spectrum analyzer output signal.

3.2.3 Experimental Results

In the sequence of experimental results below, the spectrum analyzer output was recorded as a function of several parameters, including PZT drive voltage and frequency. Comparisons were made of the received spectrum using the phase-conjugate return beam as the probe, and contrasting this with a return beam derived from a retroreflecting array, flat mirror, and cat's eye corner-cube optical system; the latter passive optical elements basically redirected the beam back toward the scattering cell, with global tilts removed, but with differential phase shifts (both in space and time) uncompensated. Prior to discussing the results, we describe the scattering cell in some detail.

For this proof-of-principle demonstration, a scattering cell was fabricated with parameters that, in essence, "match" the spatial and temporal response of the existing conjugator. Several candidate cells were tested with a variety of colloidal scattering media, including glass beads, polystyrene spheres, and silvered paint flakes. Metallic coatings were used to enhance the reflectivity of the scattering sites, as were larger scattering media such as metallic spheres (precision ball bearings), silvered craft beads, and silver nonpareils such as those used for cake decorations. The scattering particles were either suspended in the liquid via internal buoyant forces or were supported by individual strands of fine thread-like string so that they could be clustered and concentrated in the path of the interrogation probe beam. The host liquids ranged from low viscosity liquids such as water and alcohol to relatively such as glycerin, optical epoxy, FC-70, and hair gel. The latter basically created a static

suspension, which was suitable for evaluating the incident optical power necessary to achieve conjugation without optically damaging the cell constituents, for a given the scattering-site reflectivity, density and fill factor. The cells were typically 1 cm to 10 cm in length, and were cylindrical in shape. Therefore, they resembled a mild cylindrical lens so far as the side-scattered light gathering optical system is concerned. In the case of small-diameter scattering sites (5 to 50 μm diameter polystyrene spheres) the cell was periodically removed from its fixture and mildly agitated to minimize settling of the suspension during the measurement. In the case of the large-diameter sites (≈ 1 to 3 mm diameter glucose spheres), the scattering sites remained relatively stationary, with no discernible settling during the measurements. However, care was taken to collect scatter from at least three sites so that the conjugator response to independent motion was included in the experiment.

Two conjugator geometries were considered: a self-pumped "cat" conjugator, and the so-called "kitty" conjugator. The former architecture requires only a single beam: that whose wavefront-reversed replica is sought. The latter scheme requires two input beams: one beam to initiate the cat-conjugator action (this provides a pair of phase-conjugate pump beams), and a second beam, which, in this case, is the "probe beam" which scattered from the cell. The cat conjugator is self-pumped, while the kitty conjugator is pumped by an independent strong beam. In the kitty conjugator the phase is referenced to the strong beam. Because of this, the ideal kitty conjugator will conjugate the signal from all particles within its bandwidth — including global and differential Doppler-shifted particles — and can therefore not be of use in the present remote sensor approach (since all useful information will be "negated" by its action). By contrast, the self-pumped cat conjugator is self-referencing in phase, and can thus respond to a collection of particles moving at the same velocity. This response to global motion is the essential feature that comprises the remote sensor concept. A drawback to the cat conjugator is that the intensity needs to be relatively high for a reasonable conjugator response time (the response scales inversely with intensity, with about 1 second of response per watt per square cm). We turned up the incident intensity of the laser to give a roughly 100 ms response time in the conjugator, and used the viscosity of the scattering host media to slow the particle motion down to this level.

Interestingly, the conjugator can be viewed as an adaptive, narrowband, spectral filter, which processes (i.e., conjugates) only that portion of the incident Doppler-broadened spectrum which is within its bandwidth. Therefore, for a large input spectrum, the conjugated light will be significantly narrowed — with a concomitant loss of photons — by virtue of this limited frequency response. The input optical intensity can, of course, be increased to enable processing of more photons on the "wings" of the spectrum.

Typical experimental results are shown in Figures 19 (a and b). In this data run, a pair of spectra is presented for a given set of experimental conditions. Shown is the received spectrum for the case of a nonconjugate probe and a conjugate probe, respectively, after double-passing the suspension. For this experiment, a suspension of spherical objects, freely and independently supported by fine-thread-like strings in water was employed. The physical size of the scattering sites were large relative to an optical wavelength, typically in the range of 500 μm to 1 mm. For these results, a PZT was attached to the wall of the cell containing the scattering sites, at a frequency of about 28 kHz;; the laser incident power was 0.5 Watts. For the majority of the results, the signal-to-noise ratio using the conjugate beam was sufficiently high so that little or no signal averaging was required to easily discern the features in the spectrum. In contrast, the results using a retro-reflected (i.e., nonconjugate) beam required signal averaging to reveal the spectral information. For these runs, signals were averaged over 50 spectral scans. Note in the figure that the vertical scale for the nonconjugate and the conjugate spectra are different — 1 dB/div and 10 dB/div, respectively — clearly indicating the improvement in the signal-to-noise figure when employing a phase-conjugate-based sensor.

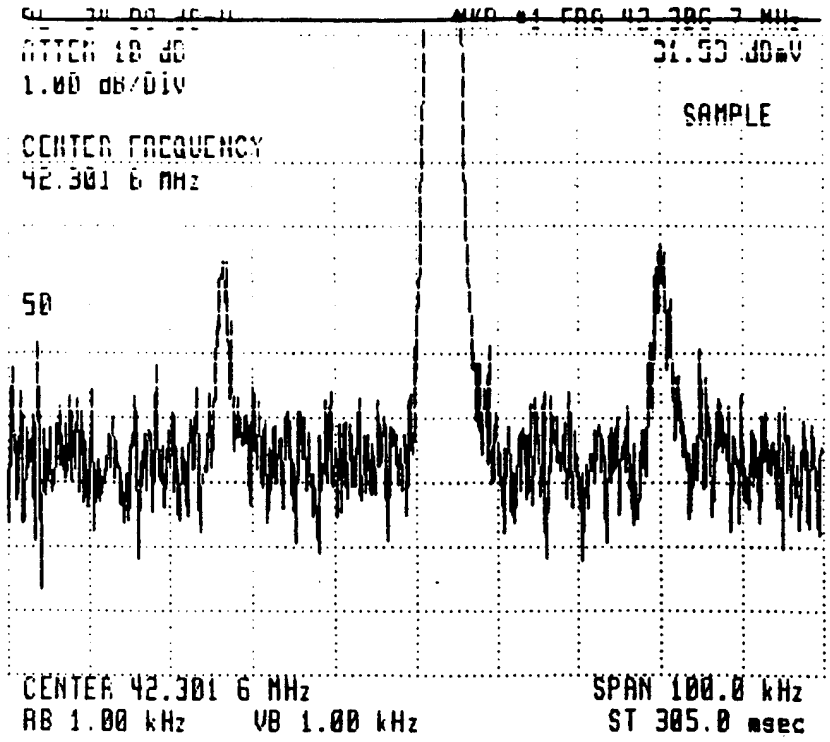

Figure 19 (a).
Experimental results of the remote sensor system in the case of suspended reflecting spheres for the case of a retroreflector. Shown is a spectrum spanning 100 kHz, centered at 42.302 MHz. A PZT at 28 kHz is attached to the cell.

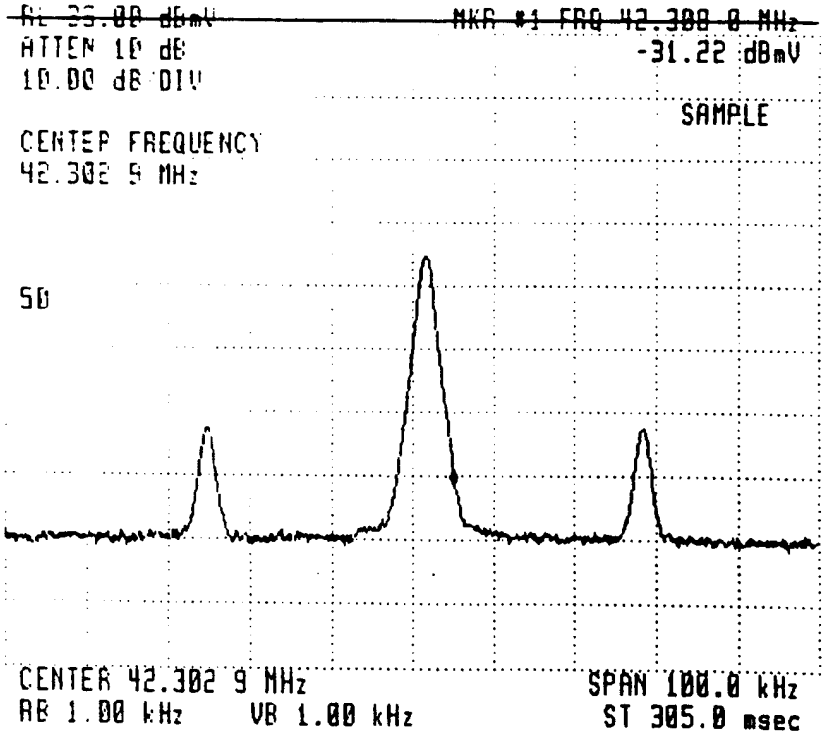

Figure 19 (b).
Experimental results of the remote sensor system in the case of suspended reflecting spheres for the case of a phase-conjugate mirror. Shown is a spectrum spanning 1 MHz, centered at 42.302 MHz. A PZT at 28 kHz is attached to the cell.

3.2.4 Summary

In both sets of data, the improvement in remote sensing performance using phase-conjugate beams in a double-pass geometry for suspended scattering sites in water is clearly shown. One can see the carrier (centered in the spectra, at 40 MHz), with a pair of sideband satellites (each at 28 kHz, on either side of the carrier). The conjugate beam has a 10 dB increase in S/N over the retro-reflected beam. This enhancement in S/N is not unlike that observed by us and others in the case of laser-based ultrasound detection from highly scattering surfaces, as compensated by a self-pumped phase conjugate mirror configuration; there, about 30 dB improvements were recorded. This greater value (compared to the 10 dB of the present study) may be attributed to two fundamental differences in the basic sensor system: (1) the present system senses motion in a suspension, where volumetric effects and differential motion are present, as compared to the single-plane, fixed scattering scenario in the ultrasound case; and (2) the present case involves a finite set of large-scale-sized scattering sites (less than 10 sites of 500 μm size) as compared to the large number of small-scale scattering sites (million sites of ≈ 1 μm size). The second point is justified experimentally since even in the nonconjugate case, a signal is seen — in the ultrasound case, the signal is buried in the noise without compensation, indicating that sufficient light is collected by our (fast) optical system with a small degree of differential phase shift. In a real-world situation — where there are a large number of distributed sites with large differential Doppler shifts — the system response is expected to be less than the background noise level without conjugation; in other words, significant improvement is expected with the use of optical conjugation in a real-world scenario.

Another benefit of this approach is that the bandwidth of the detected signal should be as narrow as the inverse of the conjugator response time; in our case, about 1/100 msec, or ≈ 10 Hz. This would allow tremendous improvements in signal to noise by permitting coherent detection with very narrow-band filtering. Unfortunately, owing to the drift in the acousto-optic modulator over the scan time of the spectrum analyzer, the expected linewidth was unable to be resolved. It would be a goal of a follow-on effort to employ higher precision drive electronics so that the narrow spectrum response can be realized, as well as to employ conjugators with faster response times so that the expected compensation benefits of this sensor system can be quantified. It would also be interesting to simulate a finite number of dynamic scattering sites with differential frequency shifts by employing a set of probe beams from a common laser source. In this manner one can impose well-defined, narrowband differential frequency shifts onto the set of probe beams via an array of PZT's or electro-optic

crystals, along with a global phase shift (on all the beams) via a PZT or a liquid crystal cell — prior to impinging the phase-conjugate mirror — so that the compensation property of the remote sensor approach can be measured directly.

4.0 RECOMMENDATIONS FOR FUTURE EFFORTS

Based on the results of our study, we offer the following progression of areas to be investigated in a follow-on effort in this area. Included are issues pertaining to the basic system components, scatter-reduction concept, communications link systems issues and, finally, remote sensor notions.

- *System components*

Consider novel devices and materials to improve the performance of each system component — both separately as well as in concert with the other elements of the overall system. For example, optical techniques should be considered to more uniformly sample the field-of-view of the optical compensation element (viz., the phase conjugator) in order to improve the spatial fidelity of the system. In addition, new nonlinear materials with spectral and temporal responses which better match those required in the scenario at hand should be considered, including other photorefractive media (e.g., semiconductors and organics) and quantum-well structures.

- *Scatter reduction*

Perform experiments using different classes of scattering candidates, as described in the background section, including absorbing sites (e.g., carbon spheres) and highly translucent dielectric particles, as well as biological media. Also, investigate the system performance in the case of highly resolvable systems (ultra-thin cells), and also in the case of controlled, distributed scattering volumes, as simulated by cascading several thin cells of varying separation, given an optical resolution bandwidth and depth of focus. Quantify the scatter reduction aspects of the phase-conjugate scheme by imaging the "shadows" of the scattering sites, as well as by measuring the wavefronts and frequency spectra of the optical beams before and after the scattering cell for both the conjugate and the nonconjugate beams. For example, good wavefront reconstruction and frequency narrowing of the Doppler-broadened spectrum are expected for the conjugate beam relative to the retroreflected beam. Moreover, perform a detailed propagation analysis of the system for a given set of scatterers and optical system parameters, so that quantitative comparisons can be made with experimental measurements.

- *Communications system*

Construct and evaluate a hybrid innovative adaptive optical system, consisting of a phase-conjugator and a conventional tilt compensation apparatus to deal with low-order errors. For example, a conventional quad detector with a pair of x-y translators (mirror galvanometers, acousto-optic or electro-optic deflectors) can be configured into a closed-loop tilt compensation apparatus. This system can also be augmented with a simple focus-error compensation system to further off-load the resultant phase error that is incident upon the conjugation element. Using this hybrid approach, global tilt errors induced by air-water interface variations as well as relative platform motion can be accommodated by the latter subsystem, while the conjugator can be most effectively dedicated to high spatial frequency, dynamic errors, including density fluctuations and wide-angle small-scale scattering. The cooperative interplay amongst these two subsystems is crucial to realizing a real-world communication link or a robust remote sensor. As an initial apparatus, one can employ cells with an air/water interface, first without scattering sites (to check to basic operation of the adaptive optical system in the face of tilt and low-order interface phase errors), followed by a sequence of experiments with the same cell, but now filled with a colloidal suspension of scattering sites. Fabricate and evaluate a retromodulator capability for the conjugator. In this manner, the ability to communicate at high data rates for the uplink can be established. When used in conjunction with the above hybrid system, a practical communication channel can be demonstrated. Coherent detection techniques can be employed to demodulate the information-bearing uplink. Demonstrate a two-way communication link by modulating the downlink as well as the uplink. Finally, demonstrate a complete system, with laser amplifiers as necessary to realize sufficient bit-error rates, adaptive optical response times and conjugator fidelity.

- *Remote sensor*

Quantify the differential frequency-shifting compensation capability of the remote sensor scheme (for a given conjugator and system scenario) by simulating an ensemble of scattering sites with an array of probe beams, each individually frequency shifted, and all with a global frequency shift from an additional device. Liquid crystal cells, PZT's, or electro-optic, or acousto-optic modulators can be employed for this simulation. The set of beams can then be directed onto a phase-conjugate mirror in a double-pass configuration. In this manner, quantitative compensation information can be obtained by precisely tuning the various opto-electronic shifters, along with spectrum analysis of the detected information to determine the dynamic range and response time of the remote sensor system, for a given global phase shifting set of parameters.

5.0 REFERENCES

1. See, for example, *Optical Phase Conjugation,* R.A. Fisher, ed. (Academic Press, New York, 1983);
   D.M. Pepper, in *The Laser Handbook, Vol. 4,* M.L. Stitch and M. Bass, eds. (North-Holland Press, Amsterdam, 1985).
   D.M. Pepper, *Sci. Am.* **254**, 74-83 (Jan. 1986).
2. B. Ya. Zel'dovich, V.I. Popovichev, V.V. Ragul'skii, and F.S. Faizullov, JETP Lett. **15**, 109 (1972).
3. D.M. Pepper, Appl. Phys. Lett. **86**, 1001 (1986).
4. M.L. Minden, R.A. Mullen and D.M. Pepper, 1988 CLEO. "Underwater retromodulator system using a self-pumped phase-conjugate mirror."
5. See, for example, the review by Ho, et. al, Opt. & Photon. News **4**, 23 (1993).
6. D. Peri, Opt. Comm. **67**, 409 (1988).
7. J. Feinberg and K. R. MacDonald, in *Photorefractive Materials and Their Applications II,* P. Gunter and J. P. Huignard, eds. (Springer-Verlag, New York, 1988), P. 151.
8. C. F. Bohren and D. R. Huffman, *Absorption and Scattering of Light by Small Particles* (Wiley Interscience, New York, 1981).
9. J. Feinberg, Opt. Lett. **7**, 486 (1982).
10. M.D. Levenson, Opt. Lett. **5**, 182 (1980).